Available online at www.sciencedirect.com
SCIENCE DIRECT
Precambrian Research 144 (2006) 140–165
Precambrian Research
www.elsevier.com/locate/precamres

Petrogenesis of Neoarchaean volcanic rocks of the MacQuoid supracrustal belt: A back-arc setting for the northwestern Hearne subdomain, western Churchill Province, Canada

H.A. Sandeman[a,*], S. Hanmer[b], S. Tella[b], A.A. Armitage[c], W.J. Davis[b], J.J. Ryan[d]

[a] *Northwest Territories Geoscience Office, Box 1500, 4601-B 52nd Avenue, Yellowknife, NT, Canada X1A 2R3*
[b] *Geological Survey of Canada, 601 Booth St., Ottawa, Ont., Canada K1A 0E8*
[c] *Commander Resources Ltd., 510-510 Burrard Street, Vancouver, BC, Canada V6C 3A8*
[d] *Geological Survey of Canada, Suite 101, 605 Robson St., Vancouver, BC, Canada V6H 1K2*

Received 10 February 2005; received in revised form 20 October 2005; accepted 3 November 2005

Abstract

Rocks exposed in the MacQuoid-Gibson Lakes region, northwest Hearne subdomain, western Churchill Province, Canada comprise three major lithotectonic assemblages: the Principal volcanic belt; the metasedimentary MacQuoid homocline and; the Cross Bay plutonic complex. Neoarchaean supracrustal rocks of the belt range in age from <2745 to <2672 Ma and were intruded during the interval <2689 to 2655 Ma by diverse plutonic units ranging from gabbro through syenogranite, but greatly dominated by tonalite. Volcanic rocks occur only in the Principal volcanic belt and the MacQuoid homocline, are metamorphosed to amphibolite facies and vary from rare pillowed to common massive basalt and andesite, intercalated with less abundant, thin, dacitic to rhyolitic tuffs, lavas and volcaniclastic rocks. Basalt and andesite are dominated by subalkaline, FeO^T-rich tholeiites with less common calc-alkaline rocks with higher SiO_2 contents and variable trace element contents. Felsic volcanic rocks exhibit calc-alkaline affinities and similarly diverse trace element abundances. The diverse trace element chemistry of the basalt and andesite supports their derivation from a heterogeneous mantle source(s) capable of generating MORB-, Arc-, BABB- and boninite-like rocks. Two geochemically distinct, arc-like suites were generated through contamination of the primary mantle-derived magmas either via assimilation of lower or middle tonalitic crust, or through contamination of their mantle source through subduction. Geochemical features of the felsic volcanic rocks indicate that these formed via both anatexis of crust in the amphibolite ± garnet stability field and via fractionation of more primitive progenitors in mid-upper crustal magma chambers. $\varepsilon Nd_{t=2680\,Ma}$ isotopic compositions cluster near depleted mantle, indicating that significant incorporation of older, >2700 Ma crust likely did not occur. $\varepsilon Nd_{t=2680\,Ma}$ values for three specimens, one from each of the Arc-like suites and one BABB-like basalt are slightly lower than the remainder, suggesting very minor incorporation of slightly older crust.

These features imply that the processes that generated the MacQuoid supracrustal belt required simultaneous tapping of geochemically distinct mantle reservoirs with concomitant anatexis of sialic crust (garnet stability field) and fractionation of felsic magmas in upper crustal magma chambers. Shallow water deposition of abundant volcaniclastic rocks and semipelite along with minor conglomerate and quartzite was broadly contemporaneous with this magmatism. We envisage a geodynamic setting characterized by tectonomagmatic processes similar to those of modern supra-subduction zone back-arc marginal basins such as the Sea of Japan. Therein, an extensional, back-arc setting, likely proximal to continental crust, provides an explanation for a broad swath of diverse mantle-derived rocks intercalated with less common felsic rocks as well as an abundance of immature clastic metasedimentary rocks.

Keywords: Western Churchill Province; MacQuoid belt; Archaean; Lithogeochemistry; Nd isotopes; Back-arc setting

* Corresponding author. Tel.: +1 867 669 2475; fax: +1 867 669 2725.
E-mail address: hamish_sandeman@gov.nt.ca (H.A. Sandeman).

0301-9268/$ – see front matter © 2005 Elsevier B.V. All rights reserved.
doi:10.1016/j.precamres.2005.11.001

1. Introduction

The western Churchill Province (wCP), a vast expanse of poorly known Canadian Precambrian shield, is exposed west of Hudson Bay (Fig. 1) and lies between the Paleoproterozoic Trans-Hudson orogen to the south and the Thelon-Taltson orogen to the west. The wCP and it is contained Archaean granite-greenstone terranes were originally distinguished from the adjacent Archaean Slave and Superior Provinces on the basis of prolific, regional, Paleoproterozoic K–Ar ages (Stockwell, 1982). Subsequently, using regional aeromagnetic data contrasts, and sparse supporting geological and geochemical data, Hoffman (1988) subdivided the wCP into Rae and Hearne Provinces (now termed Domains: Hanmer and Relf, 2000; Hanmer et al., 2004) along the Snowbird Tectonic Zone (Gibb et al., 1983). Mapping and lithological reconstructions by Aspler and Chiarenzelli (1996) in the southwestern Central Hearne subdomain of Nunavut, led those authors to propose that the Hearne likely formed in an ensimatic setting and represents either a collapsed marginal basin or a series of laterally accreted volcanic arc-trench systems, whereas the Rae represents the marginal, extended continental hinterland. More recently, under the auspices of the Western Churchill NATMAP Project (Hanmer and Relf, 2000), strategically located, field-based, multi-disciplinary bedrock mapping projects (ca. 100,000 scale) combined with supporting geoscience studies have demonstrated that the Hearne Domain may be divided into northwestern and central subdomains, distinguished by contrasting Archaean lithological associations and lithogeochemistry but mainly by differences in their latest Neoarchaean and, in particular, Paleoproterozoic tectono-thermal histories (Hanmer and Relf, 2000; Hanmer et al., 2004). Hence, the northwestern subdomain, containing the Archaean Angikuni, Yathkyed, MacQuoid and possibly Josephine River supracrustal belts is characterized by a greater abundance of siliciclastic metasedimentary rocks and fewer felsic to intermediate volcanic units relative to the Central Hearne subdomain to the south (Hanmer et al., 2004; Sandeman et al., 2004a). Moreover, the northwestern subdomain contains a suite of ca. 2600 Ma granitoids, major, ca. 2550–2490 Ma, ca. 1900 Ma and ca. 1830 Ma tectonometamorphic events and an abundance of ca. 1830 Ma Hudsonian granitoids, in contradistinction to the Central Hearne subdomain (Berman et al., 2000; Davis et al., 2000; Hanmer and Relf, 2000; Cousens et al., 2004; Hanmer et al., 2004).

This contribution presents lithogeochemical and Nd isotopic data for a wide range of Neoarchaean volcanic rocks from the MacQuoid supracrustal belt in the northwestern Hearne subdomain (Fig. 1: Davis et al., this volume; Hanmer et al., this volume) and constitutes a comparative and contemporaneous database for comparison with supracrustal belts exposed to the south in the Central Hearne supracrustal belt (see Hanmer et al., 2004; Davis et al., 2004; Cousens et al., 2004; Sandeman et al., 2004a,b). This database incorporates analyses of massive and pillowed basalt to andesite, as well as those for less common dacite and rhyolite. Lithogeochemistry indicates the presence of at least five mafic and four distinct felsic suites. Supporting Nd isotopic data suggest derivation of the volcanic rocks from variably depleted, predominantly juvenile Neoarchaean mantle. In conjunction with companion papers (Davis et al., this volume; Hanmer et al., this volume) we interpret the overall geodynamic setting of generation of the volcanic rocks to reflect lithospheric processes analogous to those that resulted in back-arc marginal basins such as the Lau, Mariana, Izu-Bonin, Scotia Sea and Sea of Japan basins (Wood et al., 1981; Sinton and Fryer, 1987; Volpe et al., 1987, 1988; Stern et al., 1990; Saunders and Tarney, 1991; Pouclet et al., 1994; Hawkins, 1995; Elliott et al., 1997; Gribble et al., 1998; Fretzdorff et al., 2002).

2. Geologic setting of the MacQuoid supracrustal belt

The MacQuoid supracrustal belt (MSB) is the largest of several strongly deformed supracrustal packages exposed in the northwestern Hearne subdomain that also include the Angikuni, Yathkyed and possibly Josephine River belts (Fig. 1). The Neoarchaean MSB (Figs. 1 and 2) is a composite volcanic-plutonic package containing amphibolite-grade volcanic and plutonic units ranging in age from <2745 to ca. 2655 Ma (Tella et al., 1997a,b; Hanmer et al., 1999a,b; Davis et al., this volume; Hanmer et al., this volume). The assembled supracrustal pile and their subvolcanic equivalents were intruded at <2689 to 2655 Ma by voluminous gabbro-tonalite-monzogranite plutons (Tella et al., 1997a,b; Sandeman et al., 2000; Davis et al., this volume) and at ca. 2609 Ma by potassium feldspar porphyritic granodiorite to monzogranite plutons. The rocks of the region form three major geological components including: (1) a southern, moderately northward-dipping metasedimentary rock dominated sequence termed the MacQuoid homocline (MH: Fig. 2); (2) the Principal volcanic belt (PVB: Fig. 2) that geometrically overlies the MH and consists of moderately north-dipping basaltic with less common felsic volcanic rocks and a series of syn- to

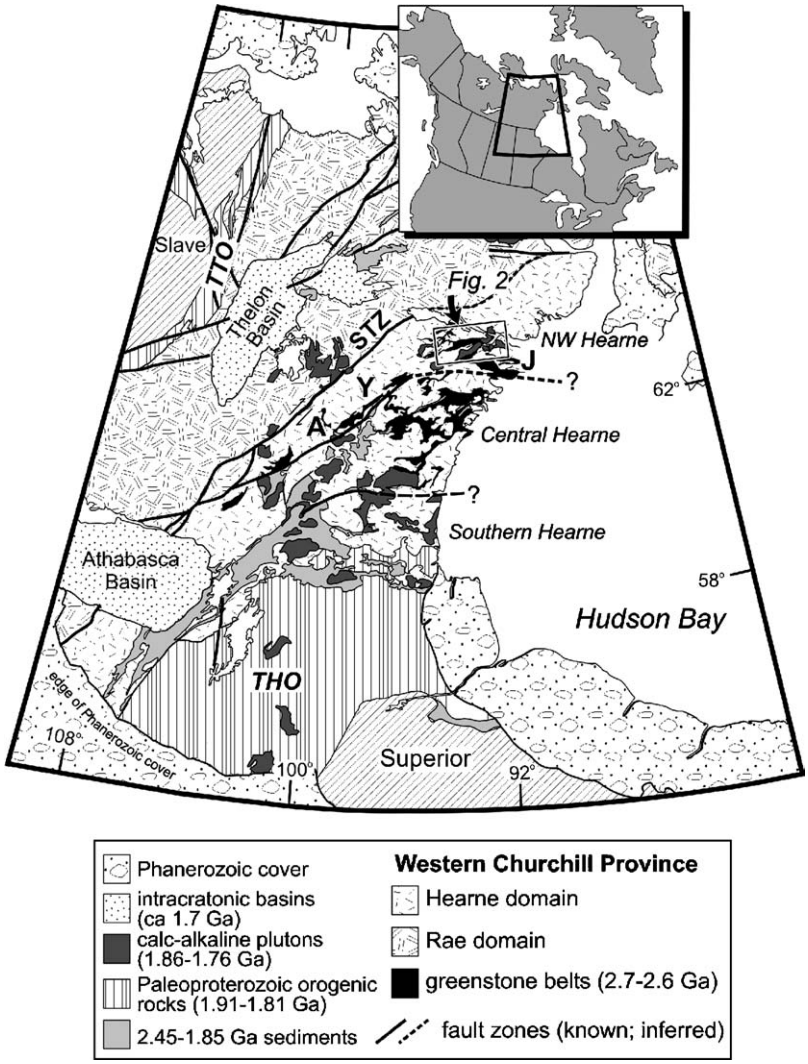

Fig. 1. Simplified geological map of north-central Laurentia showing the location of the study-area relative to the major geological provinces of the NW Canadian Shield. The subdivisions of the Hearne domain into northwest, central and southern subdomains (Hanmer and Relf, 2000; Hanmer et al., 2004) are shown as is the location of Fig. 2. Key: STZ—Snowbird Tectonic zone (Hoffman, 1988); TTO—Thelon-Taltson Orogen; THO—Trans-Hudson Orogen; J—Josephine River belt; Y—Yathkyed belt; A—Angikuni belt.

post-volcanic granodioritic to tonalitic plutons and; (3) the Cross Bay complex (CBC: Fig. 2: Hanmer et al., 1999a,b; Sandeman et al., 2000; Davis et al., this volume; Hanmer et al., this volume), a poly-deformed plutonic assemblage that is in structural contact with the Principal volcanic belt and the MaQuoid homocline, along the mylonitic Big lake shear zone (Blsz, Fig. 2: Ryan et al., 1999, 2000; Hanmer et al., this volume).

The overall outcrop pattern, relative volumes of volcanic rock types, geochronology and a discussion of the regional geology and structural evolution of the MSB are presented elsewhere (see Hanmer et al., 1999a,b; Ryan et al., 1999, 2000; Hanmer et al., this volume; Davis et al., this volume). Below, we will briefly outline the major lithological characteristics of the three major lithological components. These components (see above) and their constituent supracrustal strands (see below) form the basis for comparison and contrast of the compositional variability of the rocks of the region.

2.1. The MacQuoid homocline

The MacQuoid homocline (MH), lying immediately south of the Principal volcanic belt, is a diverse assemblage of predominantly biotite ± garnet semipelite and psammite together with subordinate laminated quartz-

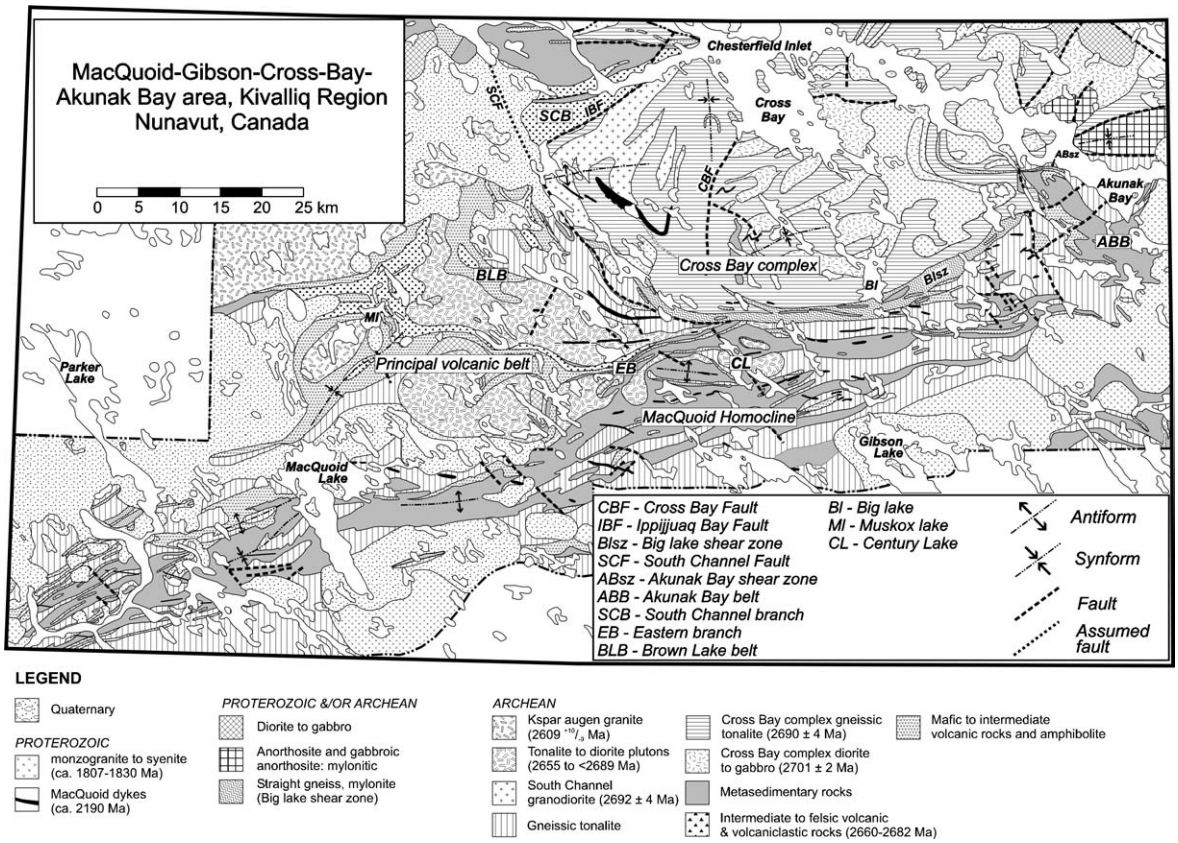

Fig. 2. Simplified geological map of the MacQuoid supracrustal belt from Parker Lake to Akunak Bay. Adapted from Tella et al. (2001).

magnetite and garnet-amphibole iron formation and garnet + aluminium silicate-bearing pelite and rare felsic volcanic rocks. Interlayered with the metasedimentary rocks are widespread, but discontinuous, generally thin (≤100 m) layer parallel units of fine- to medium-grained amphibolite. Amphibolitic intervals are well foliated and typically retain no primary textures although pillow-like features were locally observed. These units are interpreted as either mafic volcanic flows interlayered with the metasedimentary rocks or, alternatively, as transposed sills or dykes.

All of these rocks are widely intruded by tonalitic to syenogranitic intrusions, many of which are gneissose (Fig. 2: Tella et al., 1997a; Hanmer et al., 1999a). Four tonalitic rocks from the MH have been dated (Davis et al., this volume), yielding ages for homogenous tonalite plutons ranging from 2684 to 2655 Ma with one gneissic tonalite giving a maximum age of <2689 Ma.

2.1.1. The Akunak Bay belt

Lying east of the Cross Bay complex and separated from the Principal volcanic belt by a NW-trending, steeply dipping fault is the Akunak Bay belt (ABB: Fig. 2), a NW-trending, generally NE dipping package of supracrustal rocks. The belt contains abundant biotite ± garnet semipelite with rare mafic volcanic units and common layer parallel massive amphibolites and mafic dykes. To the south the belt is intruded by well-foliated tonalite and diorite plutons that are themselves cut by stocks and sheets of equigranular, typically massive, medium-grained biotite-magnetite ± fluorite monzogranite that are Paleoproterozoic in age (Peterson et al., 2002; Davis et al., this volume; Hanmer et al., this volume). On the basis of lithological similarities, including an abundance of semipelitic and pelitic units with layer parallel mafic intervals in the Akunak Bay belt, Davis et al. (this volume) suggest that it may represent a displaced correlative of the MacQuoid homocline.

2.2. The Principal volcanic belt

The Principal volcanic belt (PVB: Fig. 2) is broadly ENE-trending and extends approximately 100 km along strike, from the MacQuoid Lake area in the southwest, where the supracrustal belt is broader (ca. 25 km), to Century Lake (CL: Fig. 2) in the east where it narrows

significantly to less than 1 km and is truncated by the Big lake shear zone (Blsz: Fig. 2). In the MacQuoid Lake area, metamorphic grade is generally lowermost amphibolite facies, whereas in the east, near Big lake, metamorphic grade is middle amphibolite facies and the metavolcanic units are widely intruded by tonalite sheets. The possible eastern extension of the PVB belt along the Blsz is truncated by a NW-trending, Proterozoic(?) fault that separates it from the Akunak Bay belt lying to the NE (Davis et al., this volume). A map-scale, approximately 20 km wavelength, Paleoproterozoic, SE-verging fold of the supracrustal belt, with the Cross-Bay complex at its core (Ryan et al., 2000), has resulted in a thickened hinge zone near Muskox lake (see below) and more highly strained limbs comprising the Eastern (EB) and the South Channel branches (SCB), respectively.

Below we elaborate on the three major components of the PVB, subdivided on the basis of their geographic location, distinct lithological associations and structural styles.

2.2.1. Muskox lake

Rocks exposed in the western part of the PVB near Muskox lake (Ml: Fig. 2), include a diverse package of predominantly mafic through less abundant felsic volcanic and volcaniclastic units that locally exhibit primary volcanic textures. This area corresponds to the hinge zone of a map-scale, Proterozoic F_3 fold (regional nomenclature: Ryan et al., 1999, 2000; Hanmer et al., this volume), intruded to the north by a $2609^{+10/-9}$ Ma microcline augen granite (*sensu lato*) and to the south by a $2684^{+3/-2}$ Ma biotite + hornblende tonalite (Tella et al., 1997a; Davis et al., this volume). Mafic flows are locally pillowed but typically massive and are interlayered with both intermediate lithic and lapilli tuffs, and less abundant, massive, locally quartz porphyritic, felsic rocks interpreted as rhyolite flows. A feature common to this area as a whole is the widespread growth of decussate hornblende ($\leq$3 cm) and large ($\leq$1 cm) garnet, which overgrow and replace all primary volcanic features and deformation fabrics. Thermal ionization mass spectrometric U–Pb geochronology on zircon from an enigmatic quartz-plagioclase porphyritic felsic volcanic rock interlayered with basalt yielded a poorly defined age for the PVB at Muskox lake of <2745 Ma (Davis et al., this volume). This is interpreted as a maximum age for the PVB and, because it is ca. 60 Ma older than the majority of the U–Pb ages determined for the area (with the exception of detrital zircon ages: see Davis et al., this volume), its significance with respect to the geotectonic evolution of the MSB is poorly understood.

2.2.2. Eastern branch

The supracrustal rocks of the Eastern branch (EB) are bounded to the north by cross-cutting tonalite and diorite plutons and also by highly strained rocks of the Big lake shear zone. To the south they are in probable structural contact with rocks of the underlying MacQuoid homocline, or intruded by syn-volcanic tonalite (Davis et al., this volume; Hanmer et al., this volume). The Eastern branch (EB: Fig. 2) wraps around a large, three-lobed, tonalite pluton, between the lobes of which, its lower boundary is pinched into a pair of cusp-like keels. The EB is compositionally zoned, with predominantly mafic volcanic rocks and subvolcanic gabbro in the south and intermediate volcanic, clastic metasedimentary and minor felsic volcanic rocks in the north. Felsic tuffs and possible flows occur sporadically throughout. The mafic rocks are fine-grained, massive to layered (1–5 cm), hornblende-garnet $\pm$ clinopyroxene amphibolites, with rare, relict pillow structures. Intermediate volcanic rocks are typically fine-grained and homogeneous, but crystal, lapilli and heterolithic lithic tuffs occur locally. Metre to kilometre-scale panels of kyanite-sillimanite-andalusite-staurolite-bearing pelite, and biotite-muscovite psammite occur between panels of volcanic rocks in the eastern branch and are locally mineralized (Armitage, 1998). The majority of the metasedimentary rocks, however, tend to be monotonous and bedding is typically difficult to recognize (Davis et al., this volume). Thin (ca. 5 cm thick) quartzite layers in the psammites and a single lens of quartzite up to 10 m thick by 100 m long were noted.

2.2.3. The South Channel branch

The South Channel branch (SCB), exposed along the northwestern margin of the Cross Bay complex (SCB: Fig. 2) is a thick succession of predominantly semipelitic metasedimentary rocks and intermediate to felsic volcanic and volcaniclastic rocks with less abundant, $\leq$100 m thick mafic volcanic intervals. Overall the lithological variations observed in the SCB most closely resemble those of the MacQuoid homocline and the Akunak Bay belt. One of the felsic volcaniclastic horizons, exposed on the south side of Bowell Island (BW: Fig. 2) has been dated at ca. 2674 Ma (Z4327-HVA-K93-643: Davis et al., this volume). The intermediate to felsic volcanic rocks comprise volcaniclastic units that occur interlayered with the mafic flows. These typically comprise finely-laminated felsic crystal ash-tuffs, volcanic breccias, or massive to locally plagioclase- and hornblende-phyric panels, that parallel the regional foliation (Davis et al., this volume; Hanmer et al., this volume). Less abundant, intercalated, mafic

volcanic intervals comprise fine-grained massive amphibolites with rare preserved layering. Pillow-like features were locally observed. Featureless, massive, mafic to intermediate rocks are also abundant but it is unclear if these are sedimentary (i.e., re-worked tuffs), volcanic or hypabyssal in origin.

2.2.4. The Brown Lake belt

In the northwestern part of the map-area, lying between the Cross Bay complex and the PVB at Muskox lake is the Brown Lake volcanic belt (BLB: Fig. 2). The belt forms a roughly arcuate, NW-striking synformal panel intruded to the SW, W, E and internally by variably foliated diorite and tonalite plutons, and lies within the core of the large-scale regional, Proterozoic, F3 fold (Ryan et al., 1999, 2000; Davis et al., this volume; Hanmer et al., this volume). These rocks are well preserved in comparison to those exposed in the remainder of the region and comprise abundant massive and pillowed basalts with intercalated massive andesite and less common dacitic lithic and lapilli tuffs. They are generally at upper greenschist facies, but more commonly comprise amphibolite facies assemblages, particularly near intrusive margins. The age of the Brown Lake volcanic belt is constrained by a U–Pb TIMS zircon age of $2682^{+3/-2}$ Ma (Davis et al., this volume), for a dacitic lithic-lapilli tuff (Z5491-98TXJ-184).

2.3. The Cross Bay complex

The Cross Bay complex (CBC: Fig. 2) dominates the central-northern part of the map area and is interpreted to form a shallow bowl-like feature structurally overlying the Principal volcanic belt and MacQuoid homocline (Hanmer et al., this volume). It comprises a diverse range of plutonic rocks ranging in age from ca. 2701 to 2690 Ma (Davis et al., this volume) that are slightly older than the majority of the rocks of the MSB. The plutonic rocks range from abundant diorite and tonalite to less common monzogranite and rare gabbro, all exhibiting a well-developed, variably north- or south-dipping foliation with a strong, shallowly south- and also north northeast-plunging extension lineation (Hanmer et al., this volume). These rocks are cross-cut on their western margin by a variably foliated, microcline augen biotite monzogranite dated at 2692 ± 4 Ma (Davis et al., this volume). The CBC is bounded to the south and west by a $\leq$2 km wide zone of decimeter-scale laminated, tonalitic and granitic straight gneiss and mylonite of the Big Lake shear zone, and, to the northwest by the Ippiijuaq fault, a high strain zone separating the CBC from the South Channel branch of the MSB (see Fig. 2: Hanmer et al., 1999b; Ryan et al., 1999, 2000; Hanmer et al., this volume).

3. Geochemistry

In order to establish the compositional spectrum of volcanic rocks in the belt, a suite of geochemical samples was collected during regional traversing, from a wide range of rock-types throughout the region including greatly dominant mafic and less common intermediate and felsic volcanic and volcaniclastic rocks. These were supplemented with analyses of mafic through felsic volcanic rocks from the Eastern branch of the PVB (Armitage, 1998). Below we discuss the overall geochemical features of the volcanic rocks of the MSB including their major and trace element variations and their Nd isotopic compositions. Rocks are initially subdivided on the basis of their areal distribution (i.e., South Channel and Eastern branches, Muskox lake, the Akunak Bay and Brown Lake belts and the MacQuoid homocline). Together with the field and geochronological information presented in our companion publications (Davis et al., this volume; Hanmer et al., this volume), these geochemical data provide a foundation for further discussion of the tectonomagmatic evolution of the MacQuoid belt.

3.1. Analytical methods

Our new data-set of 54 high-precision analyses for whole-rock specimens of mafic-to-felsic volcanic and hypabyssal rocks includes specimens gathered over two field seasons (Western Churchill NATMAP, 1998, 1999). These are supplemented by less precise analyses for 39 specimens from Armitage (1998). Samples were collected from exposures throughout the map area, but the majority were obtained where volcanic rocks were abundant, and where rock exposure permitted (i.e., from the specific geographic locations described above: Fig. 2, Tables 1 and 2). Wherever possible, the cores of pillows were sampled in the mafic rocks although the preponderance of featureless, massive amphibolite-grade rocks locally made this approach difficult. Intermediate and felsic rocks were also problematic to interpret as they typically occurred as massive quartz or plagioclase porphyritic horizons of unknown origin. However, lithic tuffs and volcaniclastic debris flows were also collected and contained lithic clasts that were removed prior to final crushing and pulverization.

Approximately 1 kg of each rock sample was crushed to 5 mm-scale chips in a Braun jaw crusher and a 50 g split of each mafic rock was pulverized to a fine pow-

Table 1
Salient lithogeochemical characteristics of the volcanic rocks of the MSB

	Geog. belt	*N* (vol.%)	Mg#	Th (ppm)	Nb (ppm)	Th_N/La_N	La_N/Nb_N	La_N/Yb_N	La_N/Sm_N	Gd_N/Yb_N	Eu/Eu*	$\sum$REE (ppm)	εNd_t
Mafic													
MAF-1	Eb, ABb, Ml, BLb, MH	30 (40.5)	32–64	0.14–0.70	1.3–6.5	0.75–2.14	0.1–2.2	0.3–1.7	0.3–1.4	0.9–1.5	0.85–1.29	17–80	2.2–3.6
MAF-2	All	21 (28.4)	28–67	0.21–0.90	1.2–4.1	0.48–1.33	0.2–2.2	0.8–2.0	0.7–1.4	0.9–1.5	0.92–1.17	21–61	1.5–2.7
MAF-3	Eb, ABb, SCb, BLb	15 (20.3)	39–56	2.4–7.2	3.7–14.0	0.34–0.87	0.3–6.4	5.1–9.5	2.2–4.0	1.4–1.9	0.79–1.00	69–157	1.6
MAF-4	Eb, SCb, ABb, BLb	6 (8.1)	40–61	0.26–2.0	1.9–9.2	1.28–2.18	2.4–5.0	3.9–8.6	1.9–3.2	1.7–1.8	0.99–1.13	55–120	1.4
MAF-5	ABb, SCb	2(<1)	56–60	0.28–0.64	2.4–5.3	0.88–1.01	0.9–1.0	0.9–1.4	1.1–1.6	0.8–0.9	0.90–0.93	24–39	na
Felsic													
FEL-1	Eb, BLb	5 (26.3)	34–49	5.1–7.6	5.0–10.4	4.7–12.8	2.1–4.7	6.7–11.1	3.3–4.5	1.7–2.1	0.71–0.94	98–133	na
FEL-2	Eb	7 (36.8)	29–47	3.3–8.3	5.0–8.0	3.7–10.5	2.7–6.6	14.6–42.5	4.6–5.9	1.9–3.7	0.91–1.08	89–137	1.8
FEL-3	Eb, BLb, ABb, SCb	5 (26.2)	27–37	5.3–25.0	11.0–13.0	4.1–16.3	3.4–5.4	9.6–28.7	4.8–5.5	1.4–2.7	0.47–0.90	164–284	2.0
FEL-4	ML	2 (10.5)	22–23	23.0–27.0	15–26	7.5–15.3	0.15–0.83	3.1–7.8	3.1–4.8	0.66–0.98	0.42–0.59	21–56	na

Note: Geog. belt refers to the discrete geographic belts discussed in the text; *N* = number of samples in group; subscript N indicates values are chondrite normalized (Sun and McDonough, 1989); $Eu/Eu^* = (\sqrt{Sm_N \times Gd_N})/Eu_N$ (Taylor and McLennan, 1985); subscript *t* indicates εNd value calculated (DePaolo, 1981) at time $t = 2680$ Ma; na = not analysed. Ranges given are absolute ranges for each petrological group.

der in an agate ring mill. Felsic rocks were pulverized in a tungsten carbide mill. For analyses obtained at the Geochemical Laboratories of the Geological Survey of Canada (Ottawa), major elements and Ba were analyzed by X-Ray fluorescence analysis (XRF) of fused discs. Volatile contents, expressed as loss on ignition (LOI) were determined gravimetrically. The trace elements Ba, Co, Cr, Cu, Ni, Sc, V and Zn were analyzed by inductively coupled plasma-emission spectrometry (ICP-ES), whereas all other trace elements were determined through inductively coupled plasma-mass spectrometry (ICP-MS). Analytical errors for the data, based on the analysis of duplicates and of reference materials (SY-2, BHVO-1, PCC-1 and replicate analysis of five internal standards) are calculated at <5% relative percent for the major elements, <10% for those trace elements determined by XRF, <10% for ICP-ES analyses and <5% for ICP-MS analyses. The supplementary analyses of Armitage (1998), obtained at both Activation Laboratories (Ancaster, Ontario) and the University of Western Ontario, were determined via a number of methods including: XRF (for all major elements and some trace elements); instrumental neutron activation analysis (INAA: REE, Cs, Sc, Ta, Hf, Th and U); ICP-ES (some trace elements) and; ICP-MS (REE). Because samples collected during the 1998 and 1999 field seasons were obtained from regional, non-mineralized localities, comprised carefully cleaned, unaltered rock chips and, yielded a more precise and reproducible data-set observed in the statistical evaluation of the reference materials and duplicates (see above), we place more emphasis on the inter-element variation from our more recently obtained lithogeochemical data. This is particularly applicable in the case of the HFSE elements Nb, Y, Zr and the REE data obtained via INAA (Armitage, 1998) which show considerable scatter and jagged REE and multielement patterns.

Sm–Nd analyses were conducted at the Geochronological Laboratories of the Geological Survey of Canada (Ottawa) and analytical procedures are a variant of those documented by Thériault (1990). Whole-rock powders (ca. 0.2 g) were spiked with a ^{148}Nd–^{149}Nd mixed solution and dissolved in a warm HF–HNO_3 solution in Teflon bombs. Nd and Sm were separated using wet chemical chromatographic methods, ultra-pure acids and conventional cation specific separation resins. Isotopic ratios were determined by Thermal Ion Mass Spectrometry using a Finnigan Mat 261 solid source mass spectrometer run in the static mode. Neodymium isotopic compositions were normalized to $^{146}Nd/^{144}Nd = 0.7219$ and corrected to La Jolla $^{143}Nd/^{144}Nd = 0.511860$. Repeated analysis of an AMES standard Nd metal solution

Table 2
Lithogeochemical data for 19 representative basaltic, andesitic and felsic volcanic rocks from all major geochemical groups exposed in the MacQuoid supracrustal belt

	Sample									
	98J131b MAF-1[a] P[b] 423521[c] 7057878[d] 15[e]	98H066 MAF-1[a] P[b] 431772[c] 7068229[d] 15[e]	98M126 MAF-1[a] A[b] 465153[c] 7049819[d] 15[e]	98J099a MAF-2[a] P[b] 426443[c] 7057822[d] 15[e]	98H058 MAF-2[a] P[b] 433971[c] 7066359[d] 15[e]	98H196 MAF-2[a] A[b] 497580[c] 7062199[d] 15[e]	98H442 MAF-3[a] M[b] 434286[c] 7056377[d] 15[e]	99H043 MAF-3[a] M[b] 515245[c] 7066560[d] 15[e]	98H360 MAF-4[a] A[b] 481079[c] 7051906[d] 15[e]	98J184C MAF-4[a] LT[b] 439784[c] 7063256[d] 15[e]
SiO_2	48.00	47.70	49.30	51.40	48.51	54.10	60.70	58.80	49.70	58.90
TiO_2	0.63	0.53	1.15	0.82	0.45	0.56	0.55	0.67	0.53	0.79
Al_2O_3	15.30	20.10	13.80	13.80	18.01	21.60	15.50	16.40	15.20	16.40
FeO^T	10.62	7.29	14.67	11.70	7.38	5.58	5.22	6.75	10.53	6.20
MnO	0.19	0.16	0.23	0.25	0.19	0.19	0.10	0.10	0.16	0.10
MgO	8.10	6.55	6.63	7.30	6.83	2.60	3.08	4.79	7.98	4.01
CaO	13.51	13.63	10.56	11.23	15.14	9.91	6.36	7.60	10.39	9.35
Na_2O	1.00	1.90	2.00	1.80	1.81	3.50	2.90	3.10	3.10	2.70
K_2O	0.16	0.57	0.25	0.24	0.28	0.60	1.51	0.99	0.91	0.51
P_2O_5	0.05	0.05	0.09	0.07	0.05	0.02	0.10	0.16	0.05	0.22
LOI	2.00	1.00	0.50	0.60	0.60	1.10	3.70	0.70	0.40	0.40
Total	99.56	99.48	99.18	99.21	99.22	99.76	99.72	100.06	98.95	99.58
Mg#	58	62	45	53	62	45	51	56	58	54
Cr	400	520	180	82	540	440	85	112	141	130
Ni	180	280	70	73	290	200	71	78	167	99
Co	59	65	69	70	53	55	19	24	49	27
Sc	40	35	45	43	29	29	15	16	25	18
V	240	190	330	280	160	180	100	112	174	120
Cu	68	65	92	85	47	52	64	21	102	bd
Pb	2.0	4.1	5.0	4.2	4.0	3.0	7.0	4.0	6.0	4.0
Zn	66	73	95	82	56	65	79	97	87	41
Rb	1.7	20.0	4.2	3.2	5.8	30.0	43.0	40.0	5.4	9.4
Cs	0.55	3.30	0.14	0.04	0.97	2.80	2.40	4.60	0.07	0.51
Ba	20	120	43	120	44	140	368	310	110	130
Sr	100	230	83	86	200	140	180	200	330	320
Ga	14	17	17	16	15	15	16	17	16	18
Ta	bd	bd	bd	bd	bd	bd	0.41	0.53	0.12	0.60
Nb	1.3	1.3	2.9	1.8	1.2	1.5	5.0	7.8	1.9	8.3
Hf	0.85	0.94	1.8	1.1	0.87	1.0	2.7	3.8	0.91	3.7
Zr	33	38	60	48	30	35	123	160	29	175
Y	16	15	26	20	13	8.3	15	19	11	21
Th	0.15	0.16	0.28	0.35	0.23	0.36	3.50	3.10	0.51	2.0
U	0.04	0.07	0.08	0.09	0.07	0.10	0.77	0.81	0.11	0.57
La	1.80	2.80	3.30	2.91	2.52	2.70	14.0	16.0	9.1	21.0
Ce	4.80	6.60	8.91	7.19	5.80	7.11	27.0	34.0	22.0	48.1
Pr	0.77	0.98	1.41	1.10	0.81	1.02	3.20	4.10	2.80	5.62
Nd	4.20	4.60	7.70	5.70	4.03	5.30	12.0	16.0	11.0	22.0
Sm	1.40	1.30	2.52	1.81	1.22	1.41	2.70	3.40	2.40	4.30
Eu	0.60	0.68	0.93	0.75	0.56	0.55	0.80	0.96	0.78	1.50
Gd	2.00	2.00	3.61	2.69	1.81	1.70	2.60	3.30	2.20	3.82
Tb	0.38	0.37	0.71	0.51	0.32	0.28	0.41	0.53	0.33	0.62
Dy	2.50	2.30	4.00	3.10	2.11	1.80	2.40	3.10	1.90	3.39
Ho	0.56	0.49	0.93	0.75	0.46	0.32	0.50	0.63	0.38	0.74
Er	1.70	1.40	2.59	2.09	1.40	0.98	1.30	1.70	1.00	1.79
Tm	0.25	0.22	0.44	0.35	0.21	0.14	0.20	0.26	0.15	0.30
Yb	1.80	1.50	2.90	2.30	1.40	0.96	1.40	1.80	0.99	1.79
Lu	0.25	0.23	0.45	0.33	0.22	0.15	0.20	0.29	0.16	0.31

Table 2 (*Continued*)

	Sample									
	98H329	99H175A	98TX242A	98H326	98H443	98H007	98TX242B	98J184B	98TX076A	98J202A
	MAF-5[a]	MAF-5[a]	FEL-1[a]	FEL-1[a]	FEL-2[a]	FEL-2[a]	FEL-3[a]	FEL-3[a]	FEL-4[a]	FEL-4[a]
	A[b]	A[b]	D[b]	D[b]	Rhy[b]	LT[b]	D[b]	LT[b]	Rhy[b]	Rhy[b]
	457396[c]	520689[c]	421178[c]	458548[c]	434290[c]	441263[c]	421178[c]	439784[c]	423483[c]	426563[c]
	7092173[d]	7073221[d]	7063918[d]	7091256[d]	7056197[d]	7053585[d]	7063918[d]	7063256[d]	7059334[d]	7060678[d]
	15[e]	15[e]	15[e]	15[e]	15[e]	15[e]	15[e]	15[e]	15[e]	15[e]
SiO_2	49.9	50.9	68.20	66.10	69.20	69.30	66.60	68.80	76.00	76.90
TiO_2	0.53	0.71	0.53	0.45	0.34	0.36	0.22	0.59	0.02	0.06
Al_2O_3	13.1	13.3	13.00	15.40	14.80	14.70	16.80	14.20	13.70	13.80
FeO^T	10.53	11.16	3.90	2.43	2.43	2.71	2.43	4.86	0.50	0.72
MnO	0.20	0.21	0.09	0.07	0.05	0.03	0.04	0.07	0.07	0.07
MgO	8.76	7.80	1.62	1.79	1.22	0.80	0.54	1.10	0.08	0.12
CaO	13.35	10.55	5.65	4.10	3.18	2.77	2.20	4.59	0.85	1.00
Na_2O	1.50	2.50	3.50	4.80	4.50	4.70	5.40	3.30	4.60	4.90
K_2O	0.35	0.78	1.34	0.32	1.62	1.67	1.51	1.29	3.75	1.72
P_2O_5	0.04	0.06	0.14	0.13	0.11	0.10	0.10	0.17	0.01	0.01
LOI	1.50	1.10	2.40	2.20	2.10	1.80	1.20	0.60	0.60	0.80
Total	99.76	99.07	100.37	99.41	99.55	98.93	99.17	99.57	100.18	100.10
Mg#	60	56	43	44	47	35	28	29	22	23
Cr	320	266	68	35	39	35	12	15	bd	13
Ni	110	92	30	25	23	17	12	bd	bd	bd
Co	50	45	14	17	11	8	14	16	bd	bd
Sc	50	50	11	7.8	4.5	5.3	3.9	11	1.4	1.4
V	250	272	66	47	33	42	15	37	bd	bd
Cu	61	51	36	51	23	16	29	18	bd	bd
Pb	1.0	2.1	7.1	10.0	11.1	5.0	43.1	6.0	230	180
Zn	57	87	52	53	37	38	46	51	140	150
Rb	9.9	32.0	36.2	6.8	40.0	37.0	170	44.0	420	150
Cs	0.62	1.4	1.8	0.97	2.6	1.7	5.2	3.1	11	1.9
Ba	31	130	350	92	370	410	1477	410	56	36
Sr	63	130	160	400	250	220	830	230	53	61
Ga	13	14	13	18	20	21	18	16	24	18
Ta	0.15	0.34	0.80	0.63	0.40	0.60	0.96	1.00	1.9	1.2
Nb	2.4	5.3	10	8.0	6.7	6.0	13	11	26	15
Hf	0.95	1.3	3.3	4.2	3.3	3.8	6.7	6.2	5.2	3.9
Zr	34	49	205	171	135	158	279	314	82	101
Y	19	23	23	11	6	7	20	25	9	10
Th	0.28	0.64	6.5	3.60	8.3	4.8	25	5.3	23	27
U	0.09	0.17	1.8	0.89	2.6	1.4	8.4	1.5	30	17
La	2.30	4.62	27.0	22.0	29.0	23.0	68.0	36.0	3.7	12.0
Ce	5.20	11.00	56.2	43.0	57.0	41.0	126.0	70.0	9.0	25.1
Pr	0.78	1.51	6.2	4.7	6.3	4.3	15.0	7.7	1.0	2.8
Nd	3.70	6.49	24.1	16.0	22.0	15.0	50.0	28.1	3.4	9.4
Sm	1.30	1.89	4.4	3.0	3.2	2.5	8.0	4.8	0.76	1.6
Eu	0.48	0.67	0.98	0.89	0.80	0.77	1.9	1.4	0.10	0.28
Gd	1.9	2.7	4.2	2.4	2.2	1.9	5.6	4.7	0.69	1.3
Tb	0.38	0.51	0.73	0.35	0.27	0.28	0.74	0.71	0.12	0.23
Dy	2.70	3.41	3.91	1.80	1.22	1.3	3.6	4.0	0.78	1.1
Ho	0.63	0.78	0.79	0.35	0.21	0.24	0.63	0.89	0.19	0.26
Er	1.80	2.30	2.20	0.88	0.47	0.64	1.7	2.5	0.53	0.84
Tm	0.27	0.37	0.35	0.13	0.08	0.09	0.24	0.42	0.12	0.15
Yb	1.90	0.24	2.0	0.86	0.49	0.54	1.7	2.7	0.86	1.1
Lu	0.29	0.39	0.32	0.13	0.07	0.09	0.28	0.43	0.14	0.17

Major oxides in wt.% and trace elements in ppm. Iron is expressed as FeO^T. Major elements in wt.% oxide, trace elements in ppm. All iron is given as total FeO (FeO^T). Trace elements Co, Cr, Cu, Ni, Sc, V and Zn were obtained by ICP-ES, Ba by XRF. All remaining trace elements by ICP-MS. UTM coordinates in NAD 27 projection. Key: LOI: loss on ignition; Mg#: molecular (MgO/MgO + FeOT) × 100; bd: below detection.

[a] Group. Geochemical group according to their extended incompatible element profile (see text).

[b] Rock-type. P: pillowed flow; M: massive flow; A: amphibolite; LT: lithic tuff; D: dacite; Rhy; rhyolite.

[c] Easting.

[d] Northing.

[e] Zone.

Table 3
Nd isotopic data for 13 volcanic rocks of the MacQuoid supracrustal belt including 11 for basaltic to andesitic and 2 for dacitic to rhyolitic rocks

Sample	Volcanic group/type	Rock-type	Easting	Northing	Zone	Sm (ppm)	Nd (ppm)	$^{147}Sm/^{144}Nd$ measured	$^{143}Nd/^{144}Nd$ measured	εNd_P	εNd_t	TDM (Ma)
Mafic-intermediate												
98M126	1	A	465153	7049819	15	11.56	34.31	0.2037	0.512884 (11)	4.8	2.4	N/A
98H066	1	PB	431772	7068229	15	6.14	20.65	0.1799	0.512524 (7)	−2.2	3.6	N/A
98H031	1	A	487730	7053470	15	2.16	6.57	0.1985	0.512781 (11)	2.8	2.2	N/A
98J099A	2	PB	426443	7057822	15	9.07	26.81	0.2044	0.512880 (5)	4.7	2.1	N/A
98J131B	2	PB	423521	7057878	15	7.30	21.20	0.2081	0.512978 (12)	6.6	2.7	N/A
98H196	2	A	497580	7062199	15	6.92	23.08	0.1813	0.512494 (17)	−2.8	2.5	N/A
98H157	2	MB	457049	7053078	15	1.05	3.36	0.1878	0.512591 (9)	−0.9	2.2	N/A
98TX081	2	PB	424991	7058205	15	1.81	5.37	0.2044	0.512877 (6)	4.7	2.0	N/A
98H058	2	PB	433971	7066359	15	1.10	3.60	0.1849	0.512507 (10)	−2.6	1.5	N/A
98H301	3	MB	454136	7090404	15	4.52	21.79	0.1253	0.511459 (8)	−23.0	1.6	2760
98H320	4	A	458637	7093535	15	2.41	9.59	0.1519	0.511915 (9)	−14.1	1.4	N/A
Intermediate-felsic												
98J184B	1	LT	439784	7063256	15	4.81	26.81	0.1085	0.511178 (8)	−28.5	2.0	2726
98H007	3	LT	441263	7053585	15	2.36	14.23	0.1004	0.511026 (7)	−31.5	1.8	2735

The various parameters included herein are discussed in the text. Key: εNd_P—present day value; εNd_t—calculated to $t = 2680$ Ma; PB—pillowed basalt; MB—massive basalt; A—amphibolite; LT—dacitic lapilli tuff; UTM coordinates in NAD 27 projection. The numbers in parentheses after the measured $^{143}Nd/^{144}Nd$ are the 2σ errors $\times 10^{-6}$.

yielded $^{143}Nd/^{144}Nd = 0.512165 \pm 0.20$ (2σ). εNd values (DePaolo, 1981) were calculated using a present-day CHUR (chondritic uniform reservoir) composition of $^{143}Nd/^{144}Nd = 0.512638$ and $^{147}Sm/^{144}Nd = 0.1967$ (Jacobsen and Wasserburg, 1980). The reproducibility of the εNd values are calculated to be ca. $\pm 0.5\varepsilon$ units, whereas the reproducibility of the $^{147}Sm/^{144}Nd$ ratios is approximated at ca. 0.3%. Nd isotopic data for 13 samples are presented in Table 3.

3.2. Alteration and metamorphism

Widespread spilitization of subaqueous volcanic rocks is a common phenomenon, typically characterized by selective chemical modification including: high loss on ignition (LOI) values, scatter and inconsistency of major element data, and addition or subtraction of the large ion lithophile (LILE) elements such as Li, Rb, Sr, and Ba. Similarly, metamorphism, in particular at amphibolite or granulite facies, may result in significant element mobilization. High field strength element (HFSE) and rare earth element (REE) variations in such rocks, however, appear to reflect igneous processes and thus these elements are typically immobile under most and even extreme fluid-rock interaction (Pearce and Cann, 1973; Wood et al., 1979; Middelburg et al., 1988). Volcanic rocks of the study-area exhibit low LOI's ($\leq$3.7 wt.%) and, although LILE mobilization may be discerned in some samples, most of the major and compatible trace elements, and in particular, the HFSE and REE exhibit coherent intra- and inter-sample behavior. These observations suggest therefore that elemental variations in most specimens, and particularly in those of our new database, reflect primary igneous processes.

3.3. Major and trace element variations

For simplicity, initial discussion of the volcanic rocks is undertaken with respect to their geographic location (see above) and their bulk SiO_2 contents. The rocks are thus subdivided according to their location and into those having <63 wt.% SiO_2 (basalt to andesite) versus those with >63 wt.% SiO_2 (dacite and rhyolite). We then subdivide the rocks on the basis of their REE and multielement profiles.

Volcanic rocks of the study-area are overwhelmingly subalkaline and, in the immobile trace element discrimination diagram of Winchester and Floyd (1977: modified after Pearce, 1996: Fig. 3A) range from rare basalt through to rhyolite/dacite and trachyte. A number of samples appear to exhibit elevated Nb relative to Y and plot as alkali basalt and trachy-andesite. Many of these samples, however, are from Armitage (1998) and their anomalous compositions likely reflect less precise analyses (in particular for Nb) thereby suggesting that these rocks may not be alkaline. Major element variations suggest that the volcanic rocks of the region are calcic to calc-alkalic according to the classification of

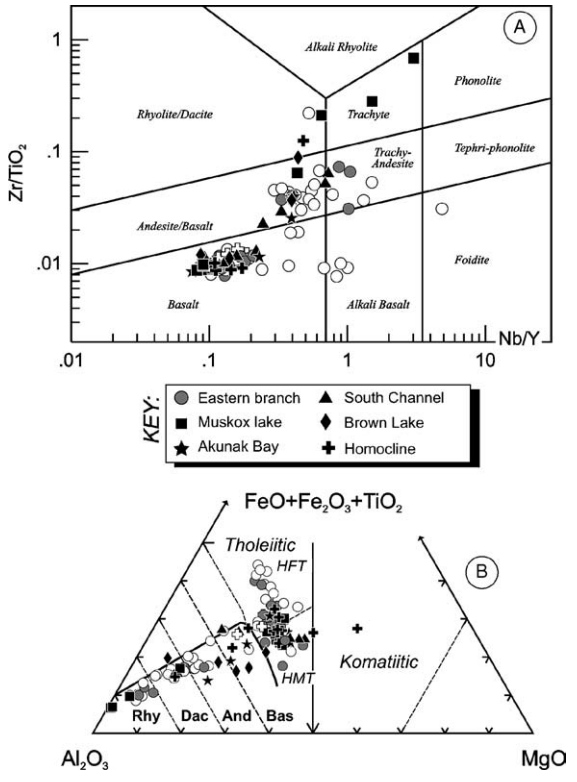

Fig. 3. (A) Zr/TiO_2 vs. Nb/Y discrimination diagram after Pearce (1996: modified from Winchester and Floyd, 1977) showing the compositions of volcanic rocks of the MSB. (B) Classification of the volcanic and volcaniclastic rocks of the MacQuoid supracrustal belt in terms of Al, Fe, Ti and Mg (Jensen, 1976). Key: Heavy line-calc alkaline/tholeiitic divide; HFT—high iron tholeiite; HMG—high magnesium tholeiite; Rhy—rhyolite; Dac—dacite; And—andesite; Bas—basalt. Open symbols are samples from Armitage (1998).

Peacock (1931), are low- to medium-K_2O (Gill, 1981) and, are dominantly tholeiitic in terms of cation percentages of Al_2O_3-FeO + Fe_2O_3 + TiO_2 (Fig. 3B: Jensen, 1976). Many of the samples (60 vol.%), particularly those from the Principal volcanic belt (EB, SCB, Ml) and the MacQuoid homocline, exhibit strong TiO_2 enrichment with increasing SiO_2, indicating that they are tholeiitic (Irvine and Barager, 1971; Miyashiro, 1974). Calc-alkaline rocks (40 vol.%), lacking FeO^T or TiO_2 enrichment with fractionation, are characterized by elevated silica contents relative to the tholeiites. Magnesium numbers (Mg#s: molecular MgO/FeO + MgO × 100: Tables 1 and 2) for the tholeiitic rocks range from 28 to 67 (mean = 50), with Cr (9–880 ppm, mean = 212 ppm) and Ni (3–290 ppm, mean = 111 ppm) contents that are typically, with few exceptions, too low for magmas that have equilibrated with modern peridotitic mantle (Roeder and Emslie, 1970). Thus, the majority of these rocks probably do not represent primitive magmas and have likely undergone fractionation in crustal magma chambers. The Mg#s (39–61: mean = 47), Cr (12–440 ppm, mean = 74 ppm) and Ni (8–200 ppm, mean = 59 ppm) contents of the calc-alkaline rocks fall within the range for those of the tholeiitic rocks, but the calc-alkaline rocks typically exhibit comparable Mg#s at higher SiO_2 (mean 58.9 wt.% versus 49.4 wt.% SiO_2) contents, presumably reflecting their lack of iron enrichment with fractionation. Intermediate and felsic volcanic rocks range from dacite through rhyolite (Fig. 3A) although a number of those of Armitage (1998) are trachy-andesite or trachyte and exhibit higher than average Nb/Y (see discussion above: Pearce, 1996). The majority of the felsic rocks exhibit unambiguous calc-alkaline, low-Fe compositions (Fig. 3B), with the exception of one transitional felsic volcanic rock from the Brown Lake belt.

Fig. 4A–F displays major and trace element trends against Mg# for the tholeiitic and calc-alkaline mafic rocks of the area. For comparison, we have shown a field for the most common, tholeiitic basaltic rocks of the Central Hearne supracrustal belt (MAF-1: Sandeman et al., 2004a). Excluding CaO, Cr, Ni, Sc and Co, the remaining major and compatible trace elements for the tholeiitic rocks exhibit negative, roughly linear or somewhat scattered trends (e.g., Fig. 4A–F), whereas the LILE elements typically show significant scatter with respect to Mg#. The majority of the HFSE and the REE, however, exhibit negative linear covariation with Mg#. Basalt and andesite of the calc-alkaline suite exhibit generally scattered or weak covariation for most elements versus Mg# and, of these, only CaO, Cr, Ni and Co shown weak positive correlation with Mg#. The HFSE and REE exhibit either weak negative or scattered covariation with Mg#. P_2O_5, Nb, Y, Zr, Hf and Ta concentrations for the rocks of the calc-alkaline suite are highly variable (e.g., ±0.3 wt.% P_2O_5 at equivalent Mg#s). Tholeiitic samples exhibit positive linear trends on Nb, Y and TiO_2 versus Zr plots (not shown: cf. Pearce and Norry, 1979), whereas calc-alkaline rocks exhibit more scattered trends with apparent decreases in Y and TiO_2 relative to the tholeiitic suite. Although it is unlikely that the rocks of each suite are cogenetic, these empirical observations suggest that the tholeiitic rocks were derived by the removal of olivine + clinopyroxene ± plagioclase from more primitive melts. Variations of these elements for the calc-alkaline rocks, however, indicate that other mineral phases, possibly hornblende, magnetite or biotite were fractionated from their primitive melts. Moreover, a pronounced variability in the abundances of the HFSE suggests that the calc-alkaline rocks are not petrogenetically linked through any simple process and hence the variability is probably a function of mantle source

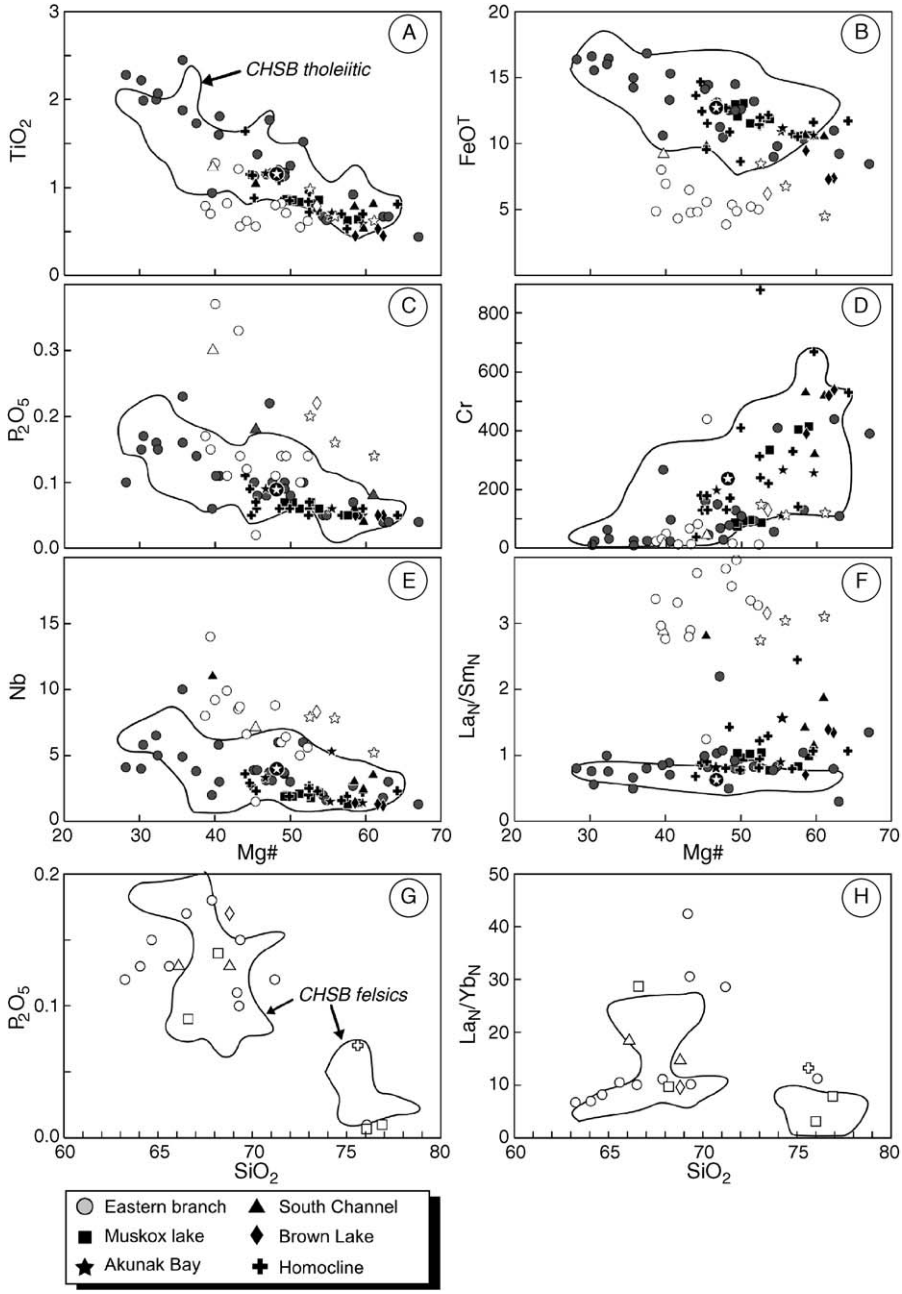

Fig. 4. A through F are plots of selected major and trace elements vs. Mg# for basaltic to andesitic volcanic and volcaniclastic rocks of the MSB. Also shown for comparison is the field for 86 tholeiitic, MORB-like volcanic rocks from the central Hearne supracrustal belt (MAF-1: Sandeman et al., 2004a) as well as the average composition for those analyses (filled circle with white star). G and H are plots of selected minor and trace elements vs. SiO_2 for dacitic through rhyolitic volcanic rocks of the MSB. Fields for two distinct types of felsic volcanic rocks of the Central Hearne supracrustal belt (Sandeman et al., 2004a: SiO_2-rich vs. SiO_2-poor), are shown for comparison. Open symbols are calc-alkaline and filled symbols are tholeiitic.

heterogeneity and/or variable amounts of crustal contamination during ascent.

The felsic rocks appear to form two distinct clusters, irrespective of their stratigraphic setting, on most bivariate plots that use SiO_2 as a fractionation index. The first is characterized by SiO_2 ranging from 63.5 to 71.2 wt.% and the second by SiO_2 >75.0 wt.% (e.g., Fig. 4G and H). Both of these groups are characterized by highly variable abundances of most elements, features which indicate that simple petrogenetic processes do not eas-

ily explain the bi-variate elemental variations of these felsic volcanic rocks. Notably, the two high SiO_2 rocks from the Muskox lake area are strongly enriched in Pb, Zn, Rb, Th and U relative to the remainder of the felsic rocks of the region (Table 2).

3.4. REE and multielement plots

Chondrite normalized REE and primitive mantle (PM) normalized (Sun and McDonough, 1989) multielement plots for selected volcanic rocks of the MSB are shown in Figs. 5 and 6 and salient lithogeochemical features of the entire database are presented in Tables 1–3. Negative P anomalies of variable magnitude are common to the mafic-intermediate rocks of the region. This is a noteworthy characteristic that is commonly observed in Archaean basaltic rocks (Ohta et al., 1996; Hollings et al., 1999; Hollings and Kerrich, 2000; Hollings, 2002; Komiya et al., 2002; Tomlinson et al., 2002; Hollings and Kerrich, 2004; Sandeman et al., 2004a), a feature we infer to result from an overestimation of the primitive mantle normalization value by Sun and McDonough (1989: cf. Sandeman et al., 2004a). Tholeiitic, basaltic to andesitic rocks are generally characterized by lower abundances of the strongly incompatible elements, relative to the calc-alkaline rocks, although some tholeiitic samples exhibit elevated large ion lithophile (LIL) and light rare earth elements (LREE). We further subdivide the basaltic to andesitic rocks into five distinct subgroups on the basis of their REE and multielement patterns (Tables 1 and 2: Fig. 5). In Fig. 5 we exclude the samples of Armitage (1998).

MAF-1 rocks predominate (40.5 vol.%: Tables 1 and 2), have generally flat to weakly LREE-depleted REE profiles, and have REE abundances ranging from 7 to 30 × chondrites. These have relatively flat PM normalized profiles with slight depletion in Th, Nb and La relative to Ce and minor, variably developed negative Ti anomalies. MAF-2 rocks (28.4 vol.%: Tables 1 and 2) are next in volumetric abundance and have flat to weakly LREE-enriched REE profiles characterized by REE abundances of 6–30 × chondrites. Their multielement patterns are similarly flat to weakly LILE and LREE-enriched, typically characterized by low abundances of the incompatible elements, but having variable negative Nb and Ti anomalies relative to the REE and Th. Negative Eu anomalies are generally minor and variable. MAF-3 rocks (20.3 vol.%) have LREE-enriched profiles with REE abundances ranging from 7 to 100 × chondrites. These rocks are characterized by fractionated multielement patterns and exhibit prominent negative anomalies in Nb, Ti and minor variable Eu anomalies and, although similar to rocks of MAF-4 (see below), are characterized by $Th_N/La_N > 1$ (Table 1). MAF-4 rocks are less abundant (8.1 vol.%: Tables 1 and 2), but like the MAF-3 rocks have LREE-enriched profiles with REE abundances ranging from 7 to 100 × chondrites. These have fractionated multielement patterns and exhibit troughs in Nb and Ti and, although broadly similar to rocks of MAF-3, are characterized by negligible Eu anomalies and significantly by $Th_N/La_N < 1$. MAF-5 rocks are rare (<1 vol.%: Tables 1 and 2) have concave-upwards REE and multielement profiles with variable negative Ti anomalies and exhibit low abundances of the REE ranging from 10 to 20 × chondrites.

Dacitic to rhyolitic rocks (Fig. 6: Tables 1 and 3) are subdivided into four distinct subgroups on the basis of their REE and multielement profiles, with all four types characterized by prominent negative P and Ti anomalies. All varieties except FEL-4 also exhibit moderate Nb troughs. FEL-1 rocks (26.3 vol.%: Tables 1 and 3) exhibit fractionated patterns with minor negative Eu anomalies, have the lowest abundances of the HREE and, have slightly positive Y anomalies (Fig. 6A and B). FEL-2 rocks are most abundant (36.8 vol.%) have extended multielement patterns similar to those of FEL-1, but are typically less fractionated, having less HREE depletion (Tables 1 and 3) and lacking positive Y and minor negative Eu anomalies (Fig. 6C and D). FEL-3 rocks (26.2 vol.%) also exhibit fractionated REE and multielement patterns and are typified by LREE-enrichment, flatter HREE segments and, variable Eu and prominent P and Ti troughs (Fig. 6E and F). FEL-4 rocks are rare (<10 vol.%) and are confined to small exposures of quartz + plagioclase porphyritic rhyolite that are interpreted as domes or flows and are exposed in the Muskox lake area of the PVB. These exhibit high Th and less so Nb relative to the LREE and do not exhibit Nb troughs. These rocks have mildly fractionated REE profiles with saucer-shaped middle to heavy REE segments and moderate negative Eu anomalies. The rocks also exhibit very prominent negative P and Ti anomalies.

3.5. Nd isotopic data

Age constraints on the formation of the volcanic rocks of the MSB are poor, in particular with respect to the timing of initial volcanism (Davis et al., this volume). For simplicity therefore, all εNd values are recalculated to 2680 Ma (Table 3), a mean age for the formation of the belt as a whole, yet well within the error of resolution of the Nd isotopic system. The samples, including basalt through rhyolite yield present day $^{144}Nd/^{143}Nd$ ratios ranging from 0.511026 to 0.512978, correspond-

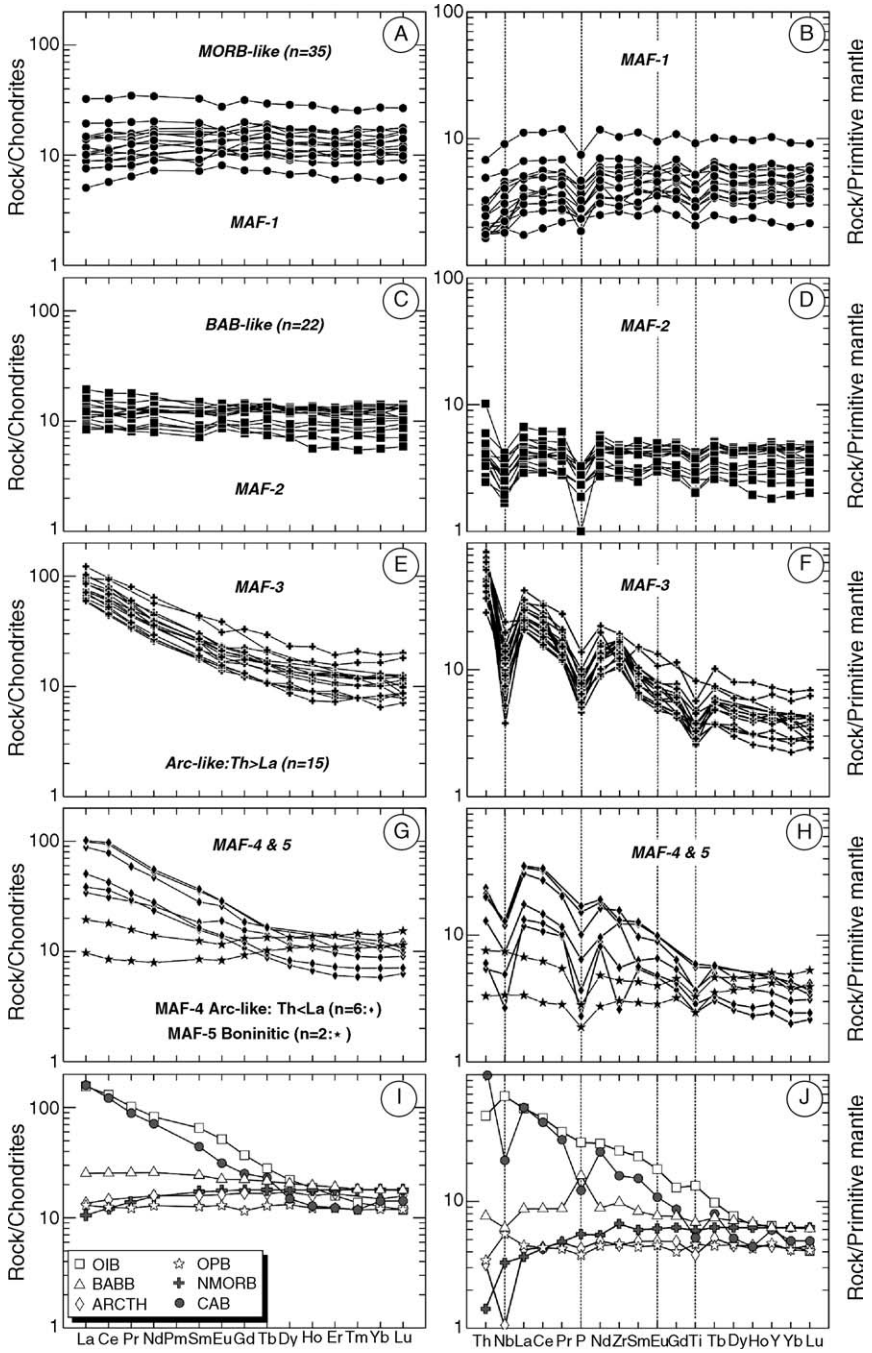

Fig. 5. A through H are chondrite normalized rare earth element and primitive mantle normalized (Sun and McDonough, 1989) multielement plots showing the profiles for the five distinct groups of basaltic to andesitic rocks of the MacQuoid supracrustal belt. I and J show representative patterns for a range of basaltic rocks from distinct Phanerozoic tectonic settings. See text for details. Key: OIB—Oceanic Island basalt (Sun and McDonough, 1989); ARCTH—Mariana arc tholeiite (GUG6; Elliott et al., 1997); BABB—back-arc basin basalt (wx-47; Fretzdorff et al., 2002); OPB—oceanic plateau basalt (average from White et al., 1999); NMORB—normal mid ocean ridge basalt (Sun and McDonough, 1989) and; CAB—average of 21 calc alkaline to transitional shoshonitic basalts from the Central Andes (Sandeman, 1995).

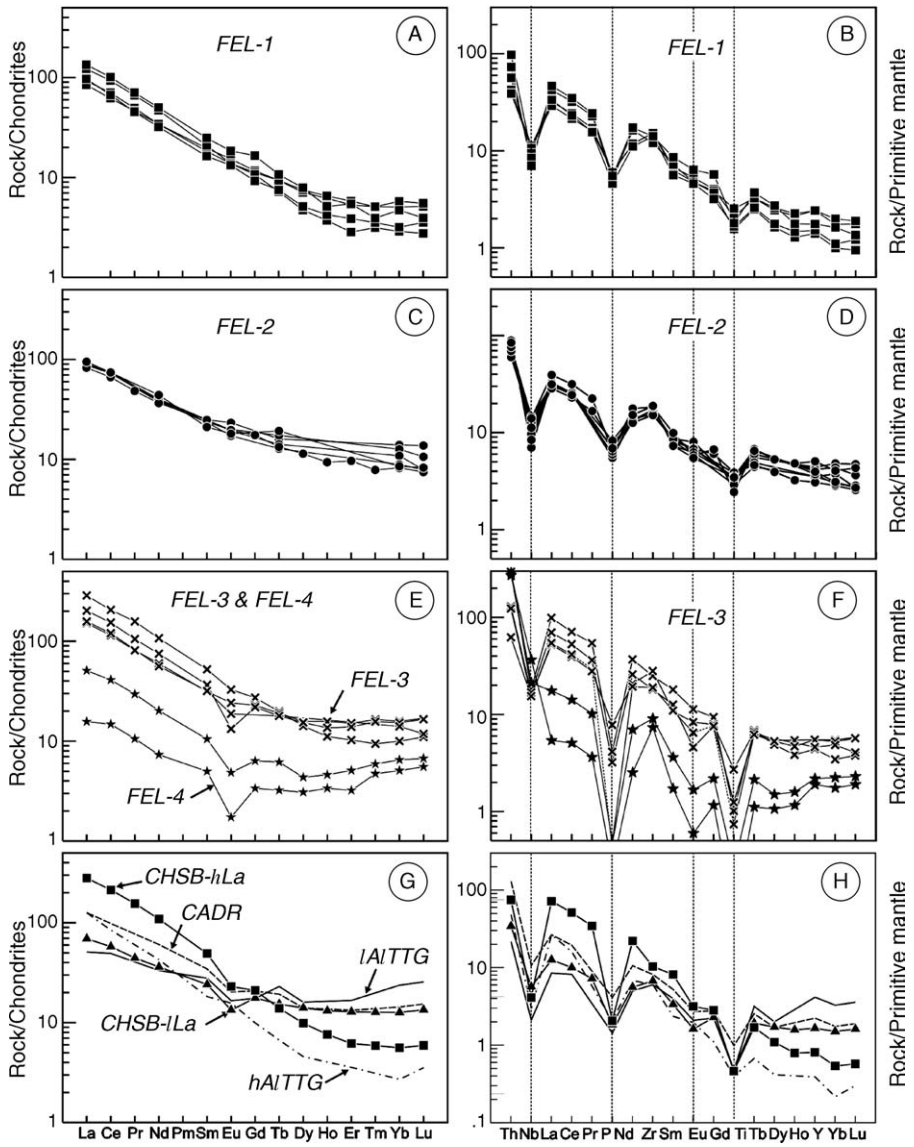

Fig. 6. A through F are chondrite normalized rare earth element and primitive mantle normalized (Sun and McDonough, 1989) multielement plots showing the profiles for the four distinct subgroups of dacitic to rhyolitic rocks of the MacQuoid supracrustal belt. Key: calc-alkaline andesite-dacite-rhyolite (CADR), low alumina tonalite-trondhjemite-granite (lAlTTG), high alumina tonalite-trondhjemite-granite (hAlTTG) (Drummond et al., 1996). Also shown are patterns for average compositions of Central Hearne supracrustal belt high-La granitoids (CHSB-hLa) and Central Hearne supracrustal belt low-La granitoids (CHSB-lLa) (Sandeman et al., 2004b).

ing to $\varepsilon Nd_{t=2680\,Ma}$ values of +1.4 to +3.6 (mean = +2.2: S.D. = 0.6: n = 13: Table 3). These data overlap, within error, and have strongly positive values commonly more depleted than the value for contemporaneous model depleted mantle (DM). Overall, their mean value is identical to that for DM ($\varepsilon NdDM_{t=2680\,Ma}$ = +2.3: DePaolo, 1981) and the standard deviation comparable to the calculated analytical, 2σ standard deviation of 0.5ε units. The two felsic rocks have $^{147}Sm/^{144}Nd$ ratios of <0.14, and yield T_{DM} values (time of removal from depleted mantle: DePaolo, 1981) of 2735 and 2736 Ma, indicating that, within the resolution of the Nd isotopic system, these samples were not derived from, nor contaminated by significantly older continental crust.

4. Discussion

Below we discuss the petrogenesis of the volcanic rocks of the MacQuoid supracrustal belt in light of the field, geochronological, lithogeochemical and Nd iso-

topic data presented herein and in our companion papers (Davis et al., this volume; Hanmer et al., this volume) and as further detailed in Tables 1–3 and Figs. 1–6. Unfortunately, because no unambiguous stratigraphic sequence was determined for the rocks of the region, the relative and precise absolute ages of the rocks are poorly known. Thus, little may be discerned about the temporal variation in lithogeochemistry and thus the relative timing of generation of the five mafic and four felsic subgroups is poorly constrained (see above: Davis et al., this volume). Of the four U–Pb zircon ages determined on the cospatial felsic volcanic rocks, one volcanic age is significantly older than the others and is a maximum (<2745 Ma: 96TXV078), whereas the remaining three U–Pb ages define a reasonably protracted, ca. 10 Ma time interval between 2682 and 2672 Ma. Within a modern context, this is a more than reasonable time span for development, evolution and accretion of a complex geotectonic assemblage.

4.1. Petrogenesis of basalt to andesite

Mafic rocks of the MSB are dominated by tholeiitic basalt that exhibits FeO^T and TiO_2 enrichment trends with increasing fractionation, and compatible element abundances that are inconsistent with them being in equilibrium with modern peridotitic mantle (Roeder and Emslie, 1970). Although age constraints are poor (see above), and it is not clear if all of the rocks are contemporaneous, the collective lithogeochemical variations of the tholeiitic rocks suggest fractionation of an assemblage including olivine + clinopyroxene, whereas depletion of the elements Sr and Eu, relative to other incompatible elements, suggests minor effects of plagioclase fractionation. In contrast, the calc-alkaline rocks exhibit more scattered bivariate element relationships, collectively characteristics that are incompatible with these rocks being related through simple petrogenetic processes and therefore implying that a number of petrological suites are likely represented. The Ti, Y, Nb, Zr interrelationships of these rocks imply the variable control on mineral/melt equilibria by minerals including olivine, clinopyroxene and plagioclase as well as phases such as amphibole, biotite and/or magnetite.

Chondrite normalized REE and primitive mantle normalized multielement plots (Sun and McDonough, 1989: Fig. 5), clearly outline five distinct subgroups (MAF-1 through 5) within the mafic rocks of the region. Predominant, tholeiitic MORB-like basalt and rare basaltic andesite of MAF-1 exhibit variable, flat, mildly LREE depleted patterns that lack HFSE troughs (excluding P see above, and to a lesser extent Ti). These rocks are the dominant mafic geochemical rock type throughout the region and are common in all of the belt segments described herein with the exception of the South Channel branch. We emphasize, however, that only six specimens from the SCB were investigated. Basaltic rocks exhibiting very similar geochemical characteristics, including flat to slightly convex-upwards REE patterns, along with minor positive and negative anomalies for Nb and Ti in multielement plots have widely been recognized to form a major component of Phanerozoic oceanic plateaux (OP) worldwide (Floyd, 1989; Kerr et al., 1997; Neal et al., 1997). The compositional similarity between Phanerozoic OP basalts and MAF-1-type Archaean basalts, typically occurring in association with komatiite in Archaean greenstone belts worldwide, has since led numerous authors to suggest that these likely formed via comparable geodynamic processes: thus, MAF-1-type rocks represent Archaean OP basalts formed above ascending plumes (Desrochers et al., 1993; Tomlinson et al., 1998, 1999; Wyman and Hollings, 1998; Kerr et al., 2000; Polat and Kerrich, 2000). Alternatively, others have suggested, on the basis of the intimate spatial and temporal association in Archaean greenstone belts of MAF-1 type basalt with both basaltic, intermediate and felsic rocks exhibiting geochemical features of tholeiitic to locally calc-alkaline arc-like compositions (Tomlinson et al., 2002; Sandeman et al., 2004a,b; Wang et al., 2004), that these belts likely formed in complex subduction zone environments that simultaneously tapped a number of mantle and crustal sources. The debate on the origin of these abundant MAF-1 Archaean basaltic rocks centres around the applicability of modern paradigms to earth processes in the Archaean, a discussion beyond the scope of this paper. What is clear, however, is that although the MSB lacks komatiite, the compositional similarity of Phanerozoic OP basalt with the MacQuoid MAF-1 rocks suggests that these either represent components of an Archaean oceanic plateau, or they represent the major constituents of “normal”, presumably thicker and hotter Archaean oceanic crust. On the basis of the evidence presented herein, we consider the latter alternative more likely and suggest that, although the MAF-1 rocks were generated via geodynamic processes comparable to those that yield Phanerozoic Oceanic plateaux, they are not Archaean oceanic plateau basalts but in fact represent Archaean analogues for the major product of partial melting of Archaean asthenospheric mantle (Archaean mid ocean ridge basalt or AMORB: cf. Ohta et al., 1996; Komiya et al., 2002; Sandeman et al., 2004a).

MAF-2 rocks comprise tholeiitic basalt with generally low abundances of the incompatible elements. These

exhibit minor LREE enrichment or depletion but have variable negative HFSE anomalies. MAF-2 rocks most closely resemble modern back-arc basin basalt (BABB) or tholeiitic arc basalt, which are widely considered to be generated through melting of strongly depleted asthenosphere with addition of a minor crustal component, potentially via contamination of the mantle source through subduction processes (Wood et al., 1981; Volpe et al., 1987, 1988; Sinton and Fryer, 1987; Stern et al., 1990; Saunders and Tarney, 1991; Pouclet et al., 1994; Hawkins, 1995; Pearce et al., 1994; Fretzdorff et al., 2002). MAF-2 rocks occur in all of the greenstone belt segments of the MSB, lending strong support to the possibility that the MacQuoid supracrustal belt likely represents the fragmented remnants of a back-arc tectonomagmatic system.

MAF-3 rocks comprise common basaltic andesite and andesite that have calc-alkaline affinities, have elevated LREE and variable HFSE troughs and, resemble arc-like mafic rocks of modern oceanic and continental margins (Pearce, 1982; Bau and Knittel, 1993; Knittel and Oles, 1994; Sandeman, 1995; Elliott et al., 1997; Gribble et al., 1998; Pearce et al., 1999). These occur throughout the MSB except at Muskox lake and in the MacQuoid homocline, and are most abundant in the Eastern branch of the Principal volcanic belt. The absence of MAF-3, arc-like rocks from Muskox lake and the MH is noteworthy and indicates that the rocks of these two areas may have formed in a tectonomagmatic setting somewhat distinct from the remainder of the supracrustal belt. Further detailed field, geochronological and lithogeochemical investigations are needed to address this issue.

Calc-alkaline basalt to andesite of MAF-4 are uncommon, but occur in all of the belt segments except for the Muskox lake area. They have elevated LREE but are characterized by low Th_N/La_N, a feature observed in continental- or ensimatic back-arc or arc-rift basalt (Barrie et al., 1993; Dostal and Mueller, 1997; Gribble et al., 1998; Hollings and Kerrich, 2000; Hollings, 2002). Th–Nb–La relationships, along with evident negative and positive Zr anomalies displayed by the MAF-4 mafic rocks, suggests that these may have experienced minor contamination via assimilation of lower crustal, Neoarchaean metagranitoids. This type of inter-element behavior appears to be a common phenomenon in basaltic rocks of many Archaean greenstone belts (Dostal and Mueller, 1997; Polat et al., 1998; Tomlinson et al., 1998, 1999, 2002; Wyman et al., 1999; Hollings and Kerrich, 2000; cf., Sandeman et al., 2004a) and likely suggests incipient rifting of pre-existing mafic crust similar to that observed in young, back-arc extensional troughs (e.g., Gribble et al., 1998; Fretzdorff et al., 2002).

MAF-5 rocks are rare, occur only in the Akunak Bay belt and South Channel branch and comprise tholeiitic basalt with concave-upwards REE and multielement patterns most similar to modern boninitic rocks. Recent models for their genesis suggest that boninites form from strongly-depleted (subjected to a prior melt extraction event), subduction zone environment asthenospheric mantle, but that the strongly depleted source was, prior to renewed melt extraction, modified through the introduction of hydrous, LILE and LREE-enriched melts (Crawford et al., 1989; Smellie et al., 1995; Falloon and Danyushevsky, 2000; MacPherson and Hall, 2001; Smithies, 2002; Boily and Dion, 2002).

In order to elaborate on the potential mantle sources for the basaltic to andesitic rocks of the region, we present (Fig. 7A–C) plots of Th/Yb versus Ta/Yb (after Pearce, 1982), La_N/Sm_N versus Th/Nb (after Elliott et al., 1997) and Ce/Nb versus Th/Nb (Saunders and Tarney, 1991). The incompatible element ratios Ta/Yb, La_N/Sm_N and Ce/Nb are useful in discriminating between variations in the incompatible element enrichment of the mantle source and less so to the amount of crustal input. Variation in the ratios Th/Yb and Th/Nb and to a lesser extent La_N/Sm_N and Ce/Nb outline differences in the crustal, or subduction zone input into the derivative magmas. These diagrams demonstrate that MAF-1 rocks, although mildly enriched in Th and Ta, are most similar to modern MORB-like mantle melts. In contrast, MAF-2 rocks have variable, but commonly mildly elevated Th relative to MAF-1, and thus approximate tholeiitic, primitive arc- or back-arc basin-like mantle melts that exhibit evidence of either crustal contamination and/or addition of "crustal" components via subduction processes. MAF-3 rocks are enriched in Th, Ta, La and Ce relative to MAF-1 and 2 rocks, suggesting that they may represent arc-like basalt generated in a mature oceanic or possibly even a continental arc setting. Thus, all of the MAF-3 rocks plot above the mantle array in Fig. 7A, the majority having incompatible element ratios similar to calc-alkaline volcanic rocks of continental arcs (cf. Pearce, 1982). Similarly, these rocks exhibit elevated Th/Nb comparable to island arc basalt and basaltic andesite and to basaltic rocks erupted onto attenuated sialic crust in a back-arc environment (e.g., the Sea of Japan: Pouclet et al., 1994). MAF-4 rocks have both high La_N/Sm_N and Ce/Nb but generally moderate Th and Ta values, features not directly comparable to volcanic rocks of intraoceanic arcs or back-arc basins (Pearce et al., 1994; Elliott et al., 1997). Their elevated La_N/Sm_N and Ta/Yb and Th/Yb suggest that they may contain a component of OIB-like mantle, however, their intermediate Th/Nb and Ce/Nb relationships

suggest that they may represent back-arc basin basalts that have assimilated crustal rocks. MAF-5 rocks have Th, La, and Ta values similar to, or slightly higher than, MAF-1 rocks suggesting that although they appear to represent depleted mantle melts, they likely have experienced a minor contribution from either contemporaneous OIB-like magmas or from crustally derived fluids or melts. We consider the latter more probable on the basis of their REE and multielement plots (see Fig. 5G and H) as these are comparable to boninites that are considered to be derived through partial melting of fluid- and silicate-melt fluxed, previously strongly depleted mantle source. Few of the mafic rocks exhibit Ta/Yb, Ce/Nb or Th/Nb compositions directly comparable to the intraoceanic Mariana arc (Elliott et al., 1997), however, they have Th/Yb, Th/Nb, La_N/Sm_N and Ce/Nb ratios comparable to rocks of the Sea of Japan, a back-arc basin formed via extension and rifting of continental crust (Pouclet et al., 1994).

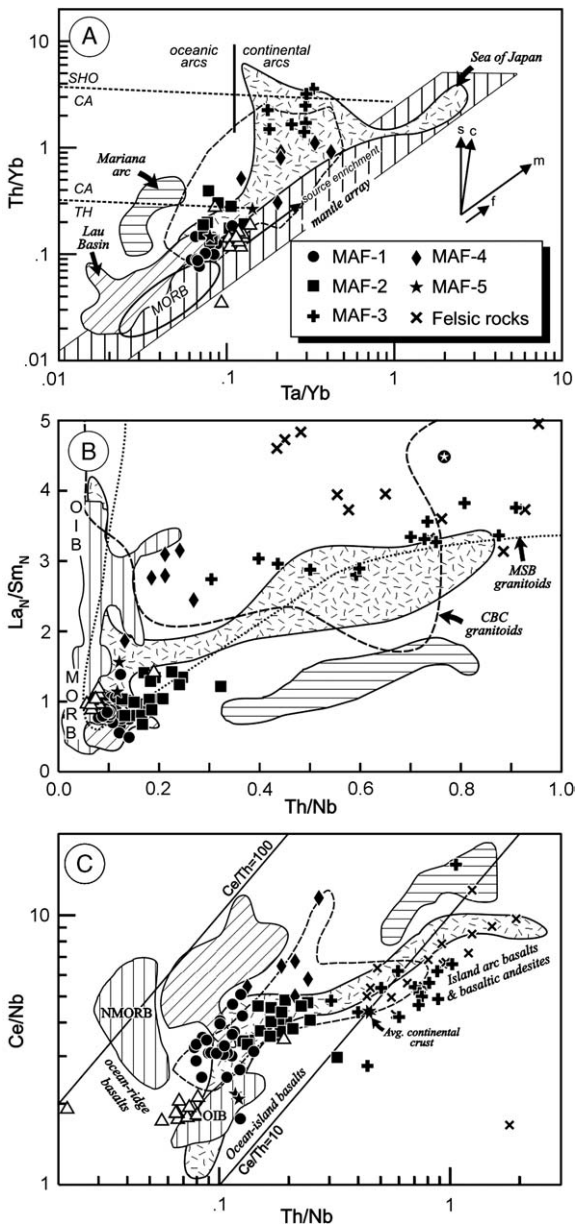

Fig. 7. Incompatible element ratio plots for volcanic rocks of the MSB. (A) Plot of Th/Yb vs. Ta/Yb (after Pearce, 1982) for basalt to andesite demonstrating their variability relative to the mantle array. Whereas the majority of the MAF-1 rocks plot close to the MORB field, many MAF-2 and MAF-4, and all MAF-3 rocks are characterized by elevated Th/Yb, comparable to volcanic rocks of modern continental arcs. The range in compositions is similar to that for rocks of the Sea of Japan. Key: dashed field is that for mafic volcanic rocks of the CHSB (Sandeman et al., 2004a); stippled field = Sea of Japan (Pouclet et al., 1994); vertical ruled field = mantle array (Pearce, 1982); horizontal ruled field = Mariana arc (Elliott et al., 1997); inclined ruled field = Lau Basin (Pearce et al., 1994) and; open triangles = the Carribean oceanic plateau (White et al., 1999). Labelled trajectories represent: s = −subduction; c = crustal contamination; m = mantle source variation; f = ca. 50% fractional crystallization of olivine + clinopyroxene + plagioclase. (B) A plot of La_N/Sm_N vs. Th/Nb (after Elliott et al., 1997) for all volcanic rocks of the MSB demonstrating their variability in Th/Nb relative to the vertical mantle array. Note that MAF-3 rocks and all felsic rocks (plotted as X's) are characterized by elevated Th/Nb, comparable to plutonic units of the MSB. (C) Ce/Nb vs. Th/Nb plot for volcanic rocks of the MSB. Symbols and fields as in A and B.

4.2. Petrogenesis of dacite and rhyolite

Intermediate to felsic volcanic and volcaniclastic rocks from the MSB exhibit calc-alkaline affinities, with the exception of one transitional specimen from the Brown Lake belt. The felsic units, irrespective of their geographic location, are characterized by non systematic variation of most elements with increasing SiO_2 suggesting that they cannot all be linked through fractional crystallization or partial melting processes.

Felsic rocks comprise four distinct subgroups on the basis of their REE and multielement patterns (Fig. 6: Table 1). FEL-1 rocks are characterized by strongly fractionated profiles with HREE depletion, by variably developed negative Nb, P and Ti anomalies and an absence of an Eu anomaly. All of these points suggest that FEL-1 felsic rocks were probably generated through partial melting of a garnet + hornblende-bearing basaltic source, likely in the lower crust (Drummond and Defant, 1990; Rapp et al., 1999; Smithies, 2000; Kamber et al., 2002). FEL-2 felsic rocks exhibit REE and multielement profiles similar to those of FEL-1, however, a higher concentration of the HREE in the FEL-2 rocks

suggests that garnet was likely absent in their source and hence, they were generated at a shallower depth, presumably as a result of the anatexis of amphibolite. These rocks also exhibit negligible Eu anomalies indicating that feldspar was not fractionated from the primary magmas. FEL-3 rocks are strongly LREE-enriched, have pronounced negative Nb, P and Ti anomalies, exhibit minor negative Eu troughs and have relatively flat HREE profiles. These likely formed through partial melting of mafic-intermediate crust in the absence of garnet, and that the magmas underwent minor fractionation of feldspar in upper crustal magma chambers. FEL-4 rocks exhibit very distinct REE and multielement profiles with high Th contents, negligible Nb but substantial P and Ti troughs and, variable negative Eu anomalies. They have minor LREE-enrichment with convex upwards REE patterns. In conjunction with their high SiO_2 contents, low cafemic element abundances and elevated economic metal concentrations, these rocks are interpreted to represent strongly fractionated felsic volcanic rocks.

Felsic rocks plotted in Fig. 7B generally fall within the extensive field defined by the granitoids of the MSB, but many fall outside of the field for the Cross Bay complex (Sandeman et al., 2000; Sandeman, unpublished data, 2005). The samples exhibit elevated La_N/Sm_N but have comparable Ce/Nb and Th/Nb relative to the silicic rocks of the Sea of Japan (Pouclet et al., 1994). These observations, along with their other geochemical characteristics indicate that these are compositionally similar to many of the calc-alkaline, ensimatic granitoids of both the MacQuoid and Central Hearne supracrustal belts (Sandeman et al., 2004b).

In Fig. 8A and B we attempt to elaborate on the processes and sources involved in the genesis of the felsic volcanic rocks of the MacQuoid belt. Fig. 8A displays the primitive mantle normalized REE patterns for representative specimens of the four felsic subgroups. These are compared to fields defined by 10% and 25%, model batch melting products from a mafic source comparable to the average composition for MAF-1 basalts (Table 4) and through application of appropriate mineral/melt partition coefficients (Martin, 1987). The REE pattern for the representative FEL-1 rock closely matches those of melts derived from garnet-bearing (25 modal% gt) amphibolite. Similarly, the REE pattern for the FEL-2 rock most closely matches those of model melts generated from batch melting of amphibolite, although the LREE contents of the FEL-2 rock are somewhat elevated relative to the model melts. The representative REE patterns for FEL-3 and 4 rocks do not match those for partial melts of mafic crustal sources.

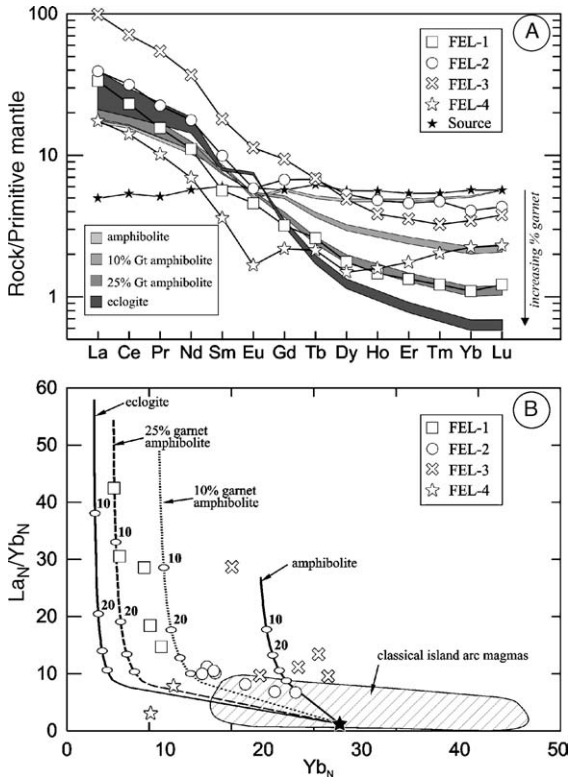

Fig. 8. (A) Primitive mantle normalized (Sun and McDonough, 1989) REE patterns for representative samples from each of the four felsic subgroups. These are compared to fields defined by 10% and 25% batch melting of average MSB MAF-1 mafic volcanic rock (source). The calculated patterns for batch melting are for potential sources comprising amphibolite, garnet (10%) amphibolite, garnet (25%) amphibolite and eclogite residues (modelled after Martin, 1987; Drummond and Defant, 1990: see Table 4). (B) Chondrite normalized La_N/Yb_N vs. Yb_N (Sun and McDonough, 1989) plot for the felsic volcanic rocks. Diagonally ruled field is for classical island arc magmas that evolve via fractional crystallization (from Drummond and Defant, 1990). Equilibrium melting curves for an average MAF-1 composition (Table 4) are shown with amphibolitic, garnet amphibolitic and eclogitic mineral residues. Labeled white dots indicate 10% increments of melting. Note that most FEL-3 samples fall to the right of the melting curves and appear to have evolved via fractional crystallization of a less evolved progenitor whereas FEL-4 rocks fall to the left of the field for classic island arc magmas and likely represent felsic rocks that have undergone extensive fractionation in the crust.

Fig. 8B outlines the distinctive REE compositions of the felsic rocks of the region in terms of their chondrite normalized La_N/Yb_N and Yb_N values. Here we show melting curves for an average composition for the most abundant mafic rocks (MAF-1) of the MSB (Table 4) with amphibolite, garnet (10 modal% gt) amphibolite, garnet (25 modal% gt) amphibolite and eclogite residual mineral assemblages. Partial melting of garnet-bearing (ca. 5–25 modal% gt) residual amphibolite assemblages can readily yield the spectrum of compositions exhib-

Table 4
Starting compositions and partition coefficients used in batch melting calculations

	Average MAF-1 mafic rock (ppm)	Clinopyroxene, cpx	Hornblende, hbl	Plagioclase, plag	Garnet, gar
La	3.42	0.1	0.2	0.13	0.04
Ce	9.50	0.2	0.3	0.11	0.08
Nd	7.72	0.4	0.8	0.07	0.20
Sm	2.69	0.6	1.1	0.05	1.00
Eu	0.99	0.6	1.3	1.30	0.98
Gd	3.39	0.7	1.8	0.04	3.8
Tb	0.67	0.7	2.0	0.037	7.5
Dy	4.15	0.7	2.0	0.031	11.0
Er	2.59	0.6	1.9	0.026	16.0
Yb	2.80	0.6	1.7	0.024	21.0
Lu	0.42	0.6	1.5	0.023	21.0

Note: Melting model residues: Eclogite = 50% cpx + 50% gar; 25% garnet amphibolite = 10% cpx + 25% gar + 50% hbl + 15% plag; 10% garnet amphibolite = 15% cpx + 10% gar + 50% hbl + 25% plag; amphibolite = 5% cpx + 30% plag + 65% hbl. Partition coefficients are from Martin (1987).

ited by the FEL-1 and possibly the FEL-2 rocks. Rocks of FEL-3 and 4, however, do not appear to be direct melts of mafic crust and likely represent fractionates of more mafic progenitors.

4.3. Implications of Nd isotopic data

In Fig. 9 we have plotted εNd_t versus chondrite normalized Th_N/Nb_N; the latter acts as a proxy for the extent of crustal contamination in mantle-derived rocks. Therein, the εNd_t and Th_N/Nb_N values for four of the five distinct varieties of basaltic to andesitic rocks (3 MAF-1, 6 MAF-2, 1 MAF-3 and 1 MAF-4 basalts: Tables 1 and 3: Fig. 9) form a fairly tight cluster and generally overlap, in terms of εNd_t, within error. The three samples of MAF-1 and one specimen of MAF-4 exhibit low, whereas those of MAF-2 and MAF-3 exhibit higher Th_N/Nb_N, suggesting that the latter compositions have been modified by Th-enriched continental crust. The two felsic rocks are characterized by comparable (within error) εNd_t but elevated Th_N/Nb_N relative to all of the mafic rocks except the one specimen of MAF-3. On this diagram we have included analyses for nine samples of plutonic rocks from the MSB (open diamonds) and for 13 plutonic rocks of the Cross Bay complex (open stars: Sandeman et al., 2000; Sandeman, unpublished data, 2005). Also shown is the mean value for Neoarchaean plutonic rocks of the Central Hearne supracrustal belt (Sandeman et al., 2004b). The DM-like $\varepsilon Nd_{t=2680\,Ma}$ values exhibited by the volcanic rocks of the MSB are therefore likely a result of their derivation from juvenile, generally LREE-depleted, mantle or crustal sources. The spread of the volcanic rock data towards the right of the mantle array may be attributed to assimilation of isotopically juvenile

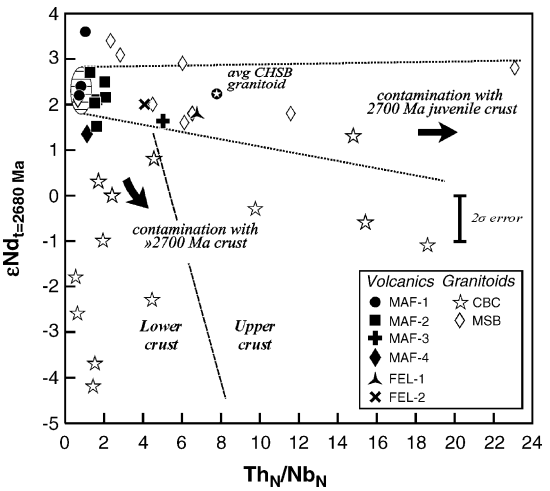

Fig. 9. $\varepsilon Nd_{t=2680\,Ma}$ vs. Th_N/Nb_N for 13 volcanic rocks from the MSB, compared to those for the plutonic units of the region (Sandeman et al., 2000). Plutonic rocks of the MSB are open diamonds and are characterized by $\varepsilon Nd_{t=2680\,Ma}$ comparable to those for the volcanic rocks. The granitoids, however, commonly have elevated Th_N/Nb_N. We also plot plutonic rocks of the Cross Bay complex (CBC: Sandeman, unpublished data, 2005) that exhibit variable, but typically significantly lower $\varepsilon Nd_{t=2680\,Ma}$ and highly variable Th_N/Nb_N relative to the volcanic and plutonic units of the MSB. Depleted mantle or MORB melts are represented by the horizontally ruled oval. An envelope and trajectory arrow are shown to demonstrate the possible effects of contamination of mantle-derived, mafic magmas with granitoid rocks of the MSB. Also shown is a trajectory arrow showing the effect of contamination of the magmas or their mantle sources with older, more isotopically evolved upper and lower continental crust. εNd results are calculated at 2680 Ma and the parameters for the calculation of Nd include: $^{143}Nd/^{144}Nd_0(CHUR) = 0.512638$; $^{147}Sm/^{144}Nd(CHUR) = 0.1967$ (Jacobsen and Wasserburg, 1980).

MSB granitoids or, alternatively, contamination of their mantle source by juvenile material through subduction processes. Because the εNd_t values for all of the volcanic rocks range from +1.4 to +3.6 (mean = +2.2), we suggest that extensive contamination via assimilation of significantly older continental crust (i.e., as apparently recorded in the Cross Bay complex rocks) is unlikely.

The MSB and it is contained granitoids formed during the interval <2745 to 2655 Ma and comprises juvenile material having Nd isotopic characteristics comparable, within error, or greater than contemporaneous depleted mantle. We suggest, therefore, that the most viable means of generating both the DM-like Nd isotopic signatures and the variable, contrasting trace element characteristics of the volcanic rocks of the MSB is through melting of asthenospheric mantle that was widely modified through the introduction of isotopically juvenile detritus via active subduction. Hence, the contrasting trace element signatures of two of the five geochemically defined mafic rock-subgroups (only two groups of mafic rocks have sufficient Nd data) are likely derived from geochemically distinct, but isotopically similar, depleted mantle sources. If crustal contamination has played a role in the genesis of these rocks, then it must have been minor, and/or predominantly involved young, juvenile Neoarchaean crust, isotopically similar to the volcanic units.

4.4. Geodynamic setting

Extensive geological mapping, a recent proliferation of precise (TIMS; single grain) and rapid (SHRIMP or LAM-ICP-MS) U–Pb geochronology along with broad-scale and detailed lithogeochemical and Nd isotopic investigations of Archaean supracrustal belts worldwide are providing new insight into the geodynamic evolution of Earth's early crust and mantle. A growing body of evidence indicates that most Archaean supracrustal belts are lithologically, temporally, lithogeochemically, and, commonly structurally, complex collages of distinct rock-types that are both like, and unlike their younger, Proterozoic and Phanerozoic counterparts (cf., de Wit, 1998; Hamilton, 1998).

Mantle plumes are now recognized to play a major role in the genesis of greenstone belts. Thus, Tomlinson and Condie (2001) summarized the results of numerous investigations and recognized three distinct types of Archaean greenstone belts that retain evidence for the role of mantle plumes including: (1) the "platform" association; (2) the "mafic-plain" association and; (3) the "arc-rift" association. All of these are typically characterized by a large proportion of pillow basalts with variable amounts of komatiite. In general, however, with the exception of the arc-rift association, felsic to intermediate volcanic rocks and clastic metasedimentary rocks are uncommon. Thus, greenstone belts containing komatiites associated with tholeiites having flat REE profiles are typically widely referred to as "plume associated". Similarly, supracrustal packages containing oceanic island basalt assemblages stratigraphically associated with variably contaminated continental and oceanic arc-like rocks have been termed arc-plume associated greenstone belts (Dostal and Mueller, 1997; Hollings and Wyman, 1999; Hollings et al., 1999; Wyman, 1999; Tomlinson and Condie, 2001; Wyman et al., 2002). Other studies describe belts that contain thick mafic volcanic assemblages dominated by tholeiites having flat REE profiles but lacking a significant ultramafic component (Hollings and Kerrich, 2000; Tomlinson and Condie, 2001; Sandeman et al., 2004a; Wang et al., 2004). In these greenstone belts, the tholeiitic basalts are unconformably overlain by, crosscut by, or locally interlayered with, arc-like basaltic to felsic volcanic rocks that are collectively intruded by a range of plutonic rocks dominated by tonalite. These diverse assemblages are inferred to represent intra-oceanic and locally continental volcanic arcs or back-arcs commonly constructed on juvenile, Neoarchaean oceanic crust.

On the basis of the evidence presented herein, and in the accompanying contributions of Davis et al (this volume) and Hanmer et al. (this volume), it is unlikely that the MacQuoid supracrustal belt represents a plume-related greenstone belt. Most significantly, ultramafic and high-MgO volcanic units have not been recognized and felsic lavas and tuffs are present (although generally subordinate) in all supracrustal strands of the MSB. Clastic metasedimentary rocks, including voluminous semipelite and psammite, similarly occur throughout the MSB whereas chemical sedimentary rocks are very rare. Geochronological data indicate that significantly older (>2700 Ma) continental crust is apparently absent, occurring only as detrital zircons in rare conglomerate.

Furthermore, even though absolute age constraints are poor, and major breaks in the MSB stratigraphy have not been recognized, lithogeochemical data indicate that the majority of the geochemical groups of mafic and felsic volcanic rocks appear to occur throughout the MH and the PVB. Felsic volcanic rocks derived through partial melting of thickened lower crust, or subducted crust in the eclogite stability field, are essentially absent whereas partial melts of garnet amphibolite crustal protoliths are relatively uncommon and occur in only two segments of the MSB. Strongly fractionated melts of amphibolitic (garnet absent) crust, however, predominate.

Geological and geochemical observations also appear to be incompatible with a classical volcanic arc localised on normal oceanic MORB-like crust above a subduction zone (see Hanmer et al., 2004; Davis et al., this volume). Although arc-like granitoid and volcanic rocks comparable in composition to those of Phanerozoic oceanic and continental arcs are common in the MSB, felsic volcanic rocks rarely form lavas and are typically subordinate whereas the voluminous plutonic units intruded relatively late in the development of the belt. Thus, the silicic volcanic and plutonic units apparently did not coalesce to form laterally extensive volcanic centres as would be expected in a classical arc setting.

An appropriate model for the MacQuoid supracrustal belt must therefore satisfy not only the lithological variations and field relationships, but also offer an explanation for the emplacement of basaltic through andesitic magmas, characterized by diverse geochemical signatures, with intercalation of less abundant, but similarly compositionally diverse felsic volcanic rocks. If the MacQuoid supracrustal belt developed in a single geodynamic setting, and all rocks are broadly contemporaneous, then this implies that the mantle yielding the mafic-intermediate volcanic rocks of the MSB was probably heterogeneous on a reasonably small-scale but was dominated by depleted sources. Thus, the widespread presence of mafic and felsic volcanic rocks having prominent negative HFSE (arc-like) anomalies with juvenile, DM-like Nd isotopic signatures, suggests that a subduction component was likely added to the sub-MSB mantle immediately prior to or during magmatic construction of the belt. Significantly, the predominantly juvenile Nd isotopic data suggests that the subduction components (contaminants) were also juvenile.

We conclude therefore that a “back-arc basin” scenario appears to be more compatible with the intimate association of petrologically diverse, contemporaneous, juvenile volcanic rocks with abundant metasedimentary units throughout the magmatic history of the MSB. This model is exemplified by the marginal back-arc basins of the Cenozoic western Pacific Ocean. These formed in response to upwelling asthenosphere in the hinterland of a subduction system. Adiabatic decompression in the upwelling mantle, together with percolation and transfer of water, LILE and possibly felsic melts from the subducting slab and the establishment of asthenospheric flow in the overlying mantle, leads to melting and back-arc spreading (cf. Saunders and Tarney, 1991). Moreover, the compositional characteristics of the erupted lavas in some back-arc basins are known to vary greatly along strike, changing from MORB-like dominated sequences in wide troughs to arc-like or arc-rift-like in narrow basins (e.g., Gribble et al., 1998). Similarly, the amount of subduction zone influence observed in the compositions of back-arc basin lavas has been demonstrated to be, at least in part, a function of distance from the active arc (Stern et al., 1990; Pearce et al., 1994; Fretzdorff et al., 2002). Thus, the lithological characteristics of the MacQuoid supracrustal belt and the variability in the chemistry of the contained volcanic rocks suggest that they may have formed in a fairly narrow, ensimatic back-arc setting, with proximal continental crust that provided predominantly isotopically juvenile sedimentary detritus (see Davis et al., this volume). Collectively, we propose that the geochemical and Nd isotopic data presented here, in conjunction with the corresponding field and geochronological data (Davis et al., this volume) constitute the primary evidence that lithospheric processes similar to those responsible for the formation of back-arc basins in the western Pacific Ocean may have operated during the development of the MSB.

4.5. Links with the Central Hearne supracrustal belt

Hanmer et al. (2004), Davis et al. (2004), Cousens et al. (2004) and Sandeman et al. (2004a,b) proposed that a large proportion of the Central Hearne subdomain lying 150 km to the south and incorporating a vast (>30,000 km^2) volcanic rock dominated supracrustal belt, was generated, during the interval 2715–2688 Ma, via lithospheric processes comparable to those that yielded the initial stages of intraoceanic arc development in the southwest Pacific (infant arc scenario: Stern and Bloomer, 1992; Hawkins, 1995; Bloomer et al., 1995). Following the infant arc stage, the establishment of a “normal” subduction zone and continuation of the attendant lithospheric-scale processes led to development of an incipient volcanic arc, characterized by the formation of spaced felsic volcanic edifices and intrusion of voluminous tonalite-granodiorite plutons (ca. 2692–2665 Ma). Although no clear geological links exist between the central and northwestern Hearne subdomains at the time of their formation, in a regional context, the proposal that the MacQuoid belt represents the poly-deformed and dispersed remnants of a ensimatic back-arc basin linked in time and space to the Central Hearne supracrustal belt, is a valid hypothesis. Moreover, the development of the rocks of the northwestern subdomain in proximity to older, Rae Domain-type crust, in contrast to the central subdomain, is suggested on the basis of U–Pb geochronological studies. Inherited (>2720 Ma) xenocrystic zircon occurs in rocks exposed in the MacQuoid, Yathkyed and Angikuni belts of the Northwestern Hearne subdomain, but is

conspicuously absent in rocks of the Central Hearne subdomain. In the Central Hearne supracrustal belt, processes associated with development of the infant-arc are inferred to have terminated during the interval ca. 2690–2686 Ma (Hanmer et al., 2004; Davis et al., 2004) with the subsequent development of an incipient ensimatic arc system. This interval corresponds, within error, with the most precise and unambiguous age for the timing of initial volcanism in the MSB at ca. 2682 Ma (Davis et al., this volume). Evolution of the MacQuoid supracrustal belt back-arc basin continued until final emplacement of late, ca. 2655 Ma tonalitic plutons.

Acknowledgments

The western Churchill NATMAP mapping crews of 1998 and 1999 are warmly thanked for assistance in sample collection. Polar Continental Shelf Project supplied helicopter logistical support in the field. R. Thériault and K. Sankowski assisted in the acquisition of Nd isotopic data. The staff of the Geochemical Laboratories at the Geological Survey of Canada, McGill University and of the Department of Earth Sciences at Memorial University of Newfoundland are thanked for the whole-rock analyses. We are grateful to Pete Hollings and Kirsty Tomlinson for providing thorough reviews of the manuscript. Ross Sherlock also provided a detailed review of an earlier version of this manuscript. This is a contribution to the Western Churchill NATMAP and is Geological Survey of Canada contribution 2004255 and Polar Continental Shelf Project contribution number 01305.

References

Armitage, A.E., 1998. Geology of the Sandhill Zn-Cu-Pb-Ag prospect and economic potential of Gibson-MacQuoid Greenstone Belt, Keewatin District, NWT, University of Western Ontario, London, Ontario, 244 pp.

Aspler, L.B., Chiarenzelli, J.R., 1996. Stratigraphy, sedimentology and physical volcanology of the Henik Group, central Ennadai-Rankin greenstone belt, Northwest Territories, Canada: late Archean paleogeography of the Hearne Province and tectonic implications. Precambrian Res. 77, 59–89.

Barrie, C.T., Ludden, J.N., Green, T.H., 1993. Geochemistry of volcanic rocks associated with Cu-Zn and Ni-Cu deposits in the Abitibi subprovince. Econ. Geol. 88, 1341–1358.

Bau, M., Knittel, U., 1993. Significance of slab-derived partial melts and aqueous fluids for the genesis of tholeiitic and calc-alkaline island-arc basalts: evidence from Mt. Arayat, Philippines. Chem. Geol. 105, 233–251.

Berman, R.G., Ryan, J.J., Tella, S., Sanborn-Barrie, M., Stern, R., Aspler, L., Hanmer, S., Davis, W., 2000. The case of multiple metamorphic events in the Western Churchill Province: evidence from linked thermobarometric and in-situ SHRIMP data, and jury deliberations. GeoCanada 2000. Geol. Ass. Canada-Min. Ass. Canada Joint Annual Meeting, Calgary, CDROM format.

Bloomer, S.H., Taylor, B., MacLeod, C.J., Stern, R.J., Fryer, P., Hawkins, J.W., Johnson, L., 1995. Early arc volcanism and the ophiolite problem: a perspective from drilling in the western Pacific. In: Active Margins and Marginal Basins of the Western Pacific, Geophysical Monograph 88, Amer. Geophys. Union.

Boily, M., Dion, C., 2002. Geochemistry of boninite-type volcanic rocks in the Frotet-Evans greenstone belt, Opatica subprovince. Precambrian Res. 115, 349–371.

Cousens, B.L., Aspler, L.B., Chiarenzelli, J.R., 2004. Dual sources of ensimatic magmas, Hearne domain, Western Churchill Province, Nunavut, Canada: Neoarchean "infant-arc" processes? Precambrian Res. 134, 169–188.

Crawford, A.J., Falloon, T.J., Green, D.H., 1989. Classification, petrogenesis and tectonic setting of boninites. In: Crawford, W.J. (Ed.), Boninites. Unwin Hyman, London, p. 465.

Davis, W., Hanmer, S., Aspler, L., Sandeman, H., Tella, S., Zaleski, E., Relf, C., Ryan, J., Berman, R., MacLachlan, K., 2000. Regional differences in the Neoarchean crustal evolution of the Western Churchill Province: can we make sense of it? GeoCanada 2000. Geol. Ass. Canada-Min. Ass. Canada Joint Annual Meeting, Calgary, CDROM format.

Davis, W., Hanmer, S., Sandeman, H.A., 2004. Temporal evolution of the Neoarchaean Central Hearne supracrustal belt: rapid generation of juvenile crust in a suprasubduction zone setting. Precambrian Res. 134, 85–112.

Davis, W.J., Hanmer, S., Tella, S., Sandeman, H.A., Ryan, J.J., this volume. U-Pb geochronology of the MacQuoid supracrustal belt and Cross Bay plutonic complex: key components of the northwestern Hearne domain, Western Churchill Province, Nunavut, Canada. Precambrian Res.

DePaolo, D.J., 1981. Neodymium isotopes in the Colorado Front Range and crust-mantle evolution in the Proterozoic. Nature 291, 193–196.

Desrochers, J., Hubert, C., Ludden, J.N., Pilote, P., 1993. Accretion of Archean oceanic fragments in the Abitibi greenstone belt, Canada. Geology 21, 451–454.

Dostal, J., Mueller, W.U., 1997. Komatiite flooding of a rifted Archean rhyolitic arc complex: geochemical signature and tectonic significance of the Stoughton-Roquemaure Group, Abitibi greenstone belt, Canada. J. Geol. 105, 545–563.

Drummond, M.S., Defant, M.J., 1990. A model for trondhjemite-tonalite-dacite genesis and crustal growth via slab melting: Archean to modern comparisons. J. Geophys. Res. 95, 21503–21521.

Drummond, M.S., Defant, M.J., Kepezhinskas, P.K., 1996. Petrogenesis of slab-derived trondhjemite-tonalite-dacite/adakite magmas. Trans. Roy. Soc. Edinb. 87, 205–215.

Elliott, T., Plank, T., Zindler, A., White, W., Bourdon, B., 1997. Element transport from slab to volcanic front at the Mariana arc. J. Geophys. Res. 102, 14991–15019.

Falloon, T.J., Danyushevsky, L.V., 2000. Melting of refractory mantle at 1.5, 2 and 2.5 GPa under anhydrous and H_2O-undersaturated conditions: implications for the petrogenesis of high-Ca boninites and the influence of subduction components on mantle melting. J. Petrol. 41, 257–283.

Floyd, P.A., 1989. Geochemical features of intraplate oceanic plateau basalts. In: Saunders, A.D., Norry, M.J. (Eds.), Magmatism in the Ocean Basins, 42. Geological Society Special Publication, pp. 215–230.

Fretzdorff, S., Livermore, R.A., Devey, C.W., Leat, P.T., Stoffers, P., 2002. Petrogenesis of the back-arc East Scotia Ridge, South Atlantic Ocean. J. Petrol. 43, 1435–1467.

Gibb, R.A., Thomas, M.D., Lapointe, P.L., Mukhopadyay, M., 1983. Geophysics of the proposed Proterozoic sutures in Canada. Precambrian Res. 19, 349–384.

Gill, J.B., 1981. Orogenic Andesites and Plate Tectonics. Springer, Berlin.

Gribble, R.F., Stern, R.J., Newman, S., Bloomer, S.H., O'Hearn, T., 1998. Chemical and isotopic composition of lavas from the northern Mariana trough: implications for magmagenesis in back-arc basins. J. Petrol. 39, 125–154.

Hamilton, W.B., 1998. Archean magmatism and deformation were not products of plate tectonics. Precambrian Res. 91, 143–179.

Hanmer, S., Tella, S., Sandeman, H.A., Ryan, J.J., Hadlari, T., Mills, A., 1999a. Proterozoic reworking in western Churchill Province, Gibson Lake-Cross bay area, Northwest Territories (Kivalliq region, Nunavut). Part I: general geology. Geol. Surv. Can. Pap. 1999-C, 55–64.

Hanmer, S., Tella, S., Sandeman, H.A., Ryan, J.J., Hadlari, T., Mills, A., 1999b. Proterozoic reworking in western Churchill Province, Gibson Lake-Cross bay area, Northwest Territories (Kivalliq region, Nunavut). Part 2: regional structural geology. Geol. Surv. Can. Pap. 1999-C, 65–75.

Hanmer, S., Relf, C., 2000. Western Churchill NATMAP Project: new results and potential significance. GeoCanada 2000. Geol. Ass. Canada-Min. Ass. Canada Joint Annual Meeting, Calgary, CDROM format.

Hanmer, S., Sandeman, H.A., Davis, W.J., Aspler, L.B., Rainbird, R.H., Peterson, T.D., Ryan, J.J., Roest, W.R., Relf, C., Irwin, D., 2004. Geology and Neoarchean tectonic setting of the Central Hearne supracrustal belt, Western Churchill Province, Nunavut, Canada. Precambrian Res. 134, 63–83.

Hanmer, S., Tella, S., Ryan, J.J., Sandeman, H.A., Berman, R.G., this volume. Late Neoarchean thick-skinned thrusting and Paleoproterozoic reworking in the MacQuoid supracrustal belt and Cross Bay plutonic complex, Western Churchill Province, Nunavut, Canada. Precambrian Res.

Hawkins, J.W., 1995. Evolution of the Lau Basin-insights from ODP Leg 135. In: Active Margins and Marginal Basins of the Western Pacific, Geophysical Monograph 88, Am. Geophys. Union.

Hoffman, P.F., 1988. United plates of America, the birth of a craton: early Proterozoic assembly and growth of Laurentia. Ann. Rev. Earth Planet. Sci. 16, 543–603.

Hollings, P., 2002. Archean Nb-enriched basalts in the northern Superior Province. Lithos 64, 1–14.

Hollings, P., Kerrich, R., 2000. An Archean arc basalt-Nb-enriched basalt-adakite association: the 2.7 Ga Confederation assemblage of the Birch-Uchi greenstone belt, Superior Province. Contrib. Mineral. Petrol. 139, 208–226.

Hollings, P., Kerrich, R., 2004. Geochemical systematics of tholeiites from the 2.86 Ga Pickle Crow assemblage, northwestern Ontario: arc basalts with positive and negative Nb-Hf anomalies. Precambrian Res. 134, 1–20.

Hollings, P., Wyman, D., 1999. Trace element and Sm-Nd systematics of volcanic and intrusive rocks from the 3 Ga Lumby Lake Greenstone belt, Superior Province: evidence for Archean plume-arc interaction. Lithos 46, 189–213.

Hollings, P., Wyman, D., Kerrich, R., 1999. Komatiite-basalt-rhyolite volcanic associations in Northern Superior Province greenstone belts: significance of plume-arc interaction in the generation of the proto continental Superior Province. Lithos 46, 137–161.

Irvine, T.N., Barager, W.R.A., 1971. A guide to the chemical classification of the common volcanic rocks. Can. J. Earth Sci. 8, 523–548.

Jacobsen, S.B., Wasserburg, G.J., 1980. Sm-Nd isotopic evolution of chondrites. Earth Planet. Sci. Lett. 50, 139–155.

Jensen, L.S., 1976. A new cation plot for classifying subalkalic volcanic rocks. Ontario Division of Mines, Misc. Pap. 66, 22 pp.

Kamber, B.S., Ewart, A., Collerson, K.D., Bruce, M.C., McDonald, G.D., 2002. Fluid-mobile trace element constraints on the role of slab melting and implications for Archaean crustal growth models. Contrib. Mineral. Petrol. 144, 38–56.

Kerr, A.C., Tarney, J., Marriner, G.F., Nivia, A., Saunders, A.D., 1997. The Caribbean-Colombian Cretaceous igneous province: the internal anatomy of an oceanic plateau. In: Mahoney, J.J., Coffin, M.F. (Eds.), Large Igneous Provinces Continental, Oceanic, and Planetary Flood Volcanism. Geophysical Monograph, vol. 88, American Geophysical Union, pp. 123–144.

Kerr, A.C., White, R.V., Saunders, A.D., 2000. LIP reading: recognizing oceanic plateaux in the geological record. J. Petrol. 41, 1041–1056.

Knittel, U., Oles, D., 1994. Basaltic volcanism associated with extensional tectonism the Taiwan-Luzon island arc: evidence for non-depleted sources and subduction zone enrichment. In: Smellie, J.L. (Ed.), Volcanism Associated with Extension at Consuming Plate Margins, Geol. Soc. Spec. Pub., vol. 81, pp. 77–94.

Komiya, T., Maruyama, S., Hirata, T., Yurimoto, H., 2002. Petrology and geochemistry of MORB and OIB in the Mid-Archean North Pole region, Pilbara Craton, Western Australia: implications for the composition and temperature of the upper mantle at 3. 5 Ga. Int. Geol. Rev. 44, 988–1016.

Macpherson, C.G., Hall, R., 2001. Tectonic setting of Eocene boninite magmatism in the Izu-Bonin-Mariana forearc. Earth Planet. Sci. Lett. 186, 215–230.

Martin, H., 1987. Petrogenesis of Archean trondhjemites, tonalites, and granodiorites from eastern Finland: major and trace element geochemistry. J. Petrol. 28, 921–953.

Middelburg, J.J., Van der Weijden, C.H., Woittiez, J.R.W., 1988. Chemical processes affecting the mobility of major, minor and trace elements during weathering of granitic rocks. Chem. Geol. 68, 253–273.

Miyashiro, A., 1974. Volcanic rock series in island arcs and active continental margins. Am. J. Sci. 274, 321–355.

Neal, C.R., Mahoney, J.J., Kroenke, L.W., Duncan, R.A., Petterson, M.G., 1997. The Ontong Java plateau. In: Mahoney, J.J., Coffin, M.F. (Eds.), Large Igneous Provinces Continental, Oceanic, and Planetary Flood Volcanism. Geophysical Monograph, vol. 88, American Geophysical Union, pp. 183–216.

Ohta, H., Maruyama, S., Takahashi, E., Watanabe, Y., Kato, Y., 1996. Field occurrence, geochemistry and petrogenesis of the Archean Mid-Oceanic Ridge Basalt (AMORBs) of the Cleaverville area, Pilbara Craton, Western Australia. Lithos 37, 199–221.

Peacock, M.A., 1931. Classification of igneous rock series. J. Geol. 39, 54–67.

Pearce, J.A., 1982. In: Thorpe, R.S. (Ed.), Trace Element Characteristics of Lavas from Destructive Plate Boundaries. John Wiley and Sons, Andesites, pp. 525–548.

Pearce, J.A., 1996. A user's guide to basalt discrimination diagrams. In: Trace element geochemistry of volcanic rocks; applications for massive sulphide exploration. Short Course Notes, Geol. Ass. Can. 12, 79-113.

Pearce, J.A., Cann, J.R., 1973. Tectonic setting of basic volcanic rocks determined using trace element analyses. Earth Planet. Sci. Lett. 19, 290–300.

Pearce, J.A., Norry, M.J., 1979. Petrogenetic implications of Ti, Zr, Y and Nb variations in volcanic rocks. Contrib. Mineral. Petrol. 69, 33–47.

Pearce, J.A., Ernewein, M., Bloomer, S.H., Parson, L.M., Murton, B.J., Johnson, L.E., 1994. Geochemistry of Lau Basin volcanic rocks: influence of ridge segmentation and arc proximity. In: Smellie, J.L. (Ed.), Volcanism Associated with Extension at Consuming Plate Margins. Geol. Soc. Spec. Pub. 81, 53–75.

Pearce, J.A., Kempton, P.D., Nowell, G.M., Noble, S.R., 1999. Hf-Nd element and isotopic perspective on the nature and provenance of mantle and subduction components in western Pacific arc-basin systems. J. Petrol. 40, 1579–1611.

Peterson, T.D., Van Breemen, O., Sandeman, H., Cousens, B., 2002. Proterozoic (1.85–1.75 Ga) igneous suites of the Western Churchill Province: granitoid and ultrapotassic magmatism in a reworked Archean hinterland. Precambrian Res. 119, 73–100.

Polat, A., Kerrich, R., 2000. Archean greenstone belt magmatism and the continental growth-mantle evolution connection: constraints from Th-U-Nb-LREE systematics of the 2.7 Ga Wawa subprovince, Superior Province, Canada. Earth Planet. Sci. Lett. 175, 41–54.

Polat, A., Kerrich, R., Wyman, D.A., 1998. The late Archean Schreiber-Hemlo and White River-Dayohessarah greenstone belts, Superior Province: collages of oceanic plateaus, oceanic arcs, and subduction-accretion complexes. Tectonophysics 289, 295–326.

Pouclet, A., Lee, J., Vidal, P., Cousens, B., Bellon, H., 1994. Cretaceous to Cenozoic volcanism in South Korea and in the Sea of Japan: magmatic constraints on the opening of the back-arc basin. In: Smellie, J.L. (Ed.), Volcanism Associated with Extension at Consuming Plate Margins. Geol. Soc. Spec. Pub. 81, 169–191.

Rapp, R.P., Shimizu, N., Norman, M.D., Applegate, G.S., 1999. Reaction between slab-derived melts and peridotite in the mantle wedge: experimental constraints at 3.8 GPa. Chem. Geol. 160, 335–356.

Roeder, P.L., Emslie, R.F., 1970. Olivine-liquid equilibrium. Contrib. Mineral. Petrol. 29, 275–289.

Ryan, J.J., Hanmer, S., Tella, S., Sandeman, H.A., 1999. Detailed structural studies, Gibson-Lake-Cross Bay-MacQuoid Lake area, Northwest Territories (Kivalliq region, Nunavut). Geol. Surv. Can. Pap. 1999-C, 87–96.

Ryan, J.J., Davis, W., Berman, R., Hanmer, S., Tella, S., Sandeman, H., 2000. Regional foliation development in the MacQuoid Lake-Gibson Lake-Akunak Bay area (Western Churchill Province): looking through Paleoproterozoic reworking at a Neoarchean orogenic event. GeoCanada 2000. Geol. Ass. Canada-Min. Ass. Canada Joint Annual Meeting, Calgary, CDROM format.

Sandeman, H.A.I., 1995. Lithostratigraphy, petrology and geochronology of the Crucero Supergroup, Puno, SE Peru: implications for the Cenozoic geodynamic evolution of the southern Peruvian Andes. Unpublished Ph.D. thesis, Queen's University, 384 pp.

Sandeman, H., Davis, W., Hanmer, S., MacLachlan, K., Peterson, T., Ryan, J., Tella, S., Cousens, B., Relf, C., 2000. Geochemistry of Neoarchean plutonic rocks of the Hearne Domain, Western Churchill Province, Nunavut: granitoids associated with the formation and stabilization of "arc-like" oceanic crust. GeoCanada 2000. Geol. Ass. Canada-Min. Ass. Canada Joint Annual Meeting, Calgary, CDROM format.

Sandeman, H.A., Hanmer, S., Davis, W.J., Ryan, J.J., Peterson, T.D., 2004a. Neoarchaean volcanic rocks, Central Hearne supracrustal belt, Western Churchill Province, Canada: geochemical and isotopic evidence supporting intraoceanic, suprasubduction zone extension. Precambrian Res. 134, 113–141.

Sandeman, H.A., Hanmer, S., Davis, W.J., Ryan, J.J., Peterson, T.D., 2004b. Whole-rock and Nd isotopic geochemistry of Neoarchaean granitoids and their bearing on the evolution of the Central Hearne supracrustal belt, Western Churchill Province, Nunavut, Canada. Precambrian Res. 134, 143–167.

Saunders, A., Tarney, J., 1991. Back-arc basins. In: Floyd, P.A. (Ed.), Oceanic Basalt. Blackie and Sons, Glasgow, UK, pp. 219–263.

Sinton, J.M., Fryer, P., 1987. Mariana trough lavas from 18 °N: implications for the origin of back arc basin basalt. J. Geophys. Res. 92, 12782–12802.

Smellie, J.L., Stone, P., Evans, J., 1995. Petrogenesis of boninites in the Ordovician Ballantrae Complex ophiolite, southwestern Scotland. J. Volcan. Geother. Res. 69, 323–342.

Smithies, R.H., 2000. The Archaean tonalite-trondhjemite-granodiorite (TTG) series is not an analogue of Cenozoic adakite. Earth Planet. Sci. Lett. 182, 115–125.

Smithies, R.H., 2002. Archaean boninite-like rocks in an intracratonic setting. Earth Planet. Sci. Lett. 197, 19–34.

Stern, R.J., Bloomer, S.H., 1992. Subduction zone infancy: examples from the Izu-Bonin-Mariana and Jurassic California arcs. Geol. Soc. Am. Bull. 104, 1621–1636.

Stern, R.J., Lin, P., Morris, J.D., Jackson, M.C., Fryer, P., Bloomer, S.H., Ito, E., 1990. Enriched back-arc basin basalt from the northern Mariana Trough: implications for the magmatic evolution of back-arc basins. Earth Planet. Sci. Lett. 100, 210–225.

Stockwell, C.H., 1982. Proposals for time classification and correlation of Precambrian rocks and events in Canada and adjacent areas of the Canadian Shield, Part 1: a time classification of Precambrian rocks and events. Geol. Surv. Can. Spec. Pa 80-19.

Sun, S.-s, McDonough, W.F., 1989. Chemical and isotopic systematics of oceanic basalt: implications for mantle composition and processes. In: Saunders, A.D., Norry, M.J. (Eds.), Magmatism in the Ocean Basins. Geol. Soc. Spec. Publ. 42, 313–345.

Taylor, S.R., McLennan, S.M., 1985. The Continental Crust: Its Composition and Evolution. Blackwell Scientific Publications, Oxford.

Tella, S., LeCheminant, A.N., Sanborn-Barrie, M., Venance, K.E., 1997a. Geology and structure of parts of the MacQuoid Lake area, District of Keewatin, Northwest Territories. In: Current Research. Geol. Surv. Can. Pap. 1997-C, 123–132.

Tella, S., LeCheminant, A.N., Sanborn-Barrie, M., Venance, K.E., 1997b. Geology, parts of MacQuoid Lake, District of Keewatin, Northwest Territories; Geol. Surv. Can. Open File 3404, scale 1:50,000.

Tella, S., Hanmer, S., Sandeman, H.A., Ryan, J.J., Mills, A., Davis, W.J., Berman, R.G., Wilkinson, L., Kerswill, J.A., 2001. Geology, MacQuoid Lake-Gibson Lake-Akunak Bay area, Nunavut; Geol. Surv. Can. Map 2008A, scale 1:100,000.

Thériault, R.J., 1990. Methods for Rb-Sr and Sm-Nd isotopic analyses at the geochronology laboratory Geological Survey of Canada. Geol. Surv. Can. Pap. 1989-2, 3–6.

Tomlinson, K.Y., Stevenson, R.K., Hughes, D.J., Hall, R.P., Thurston, P.C., Henry, P., 1998. The Red Lake greenstone belt, Superior Province: evidence of plume-related magmatism at 3 Ga and evidence of an older enriched source. Precambrian Res. 89, 59–76.

Tomlinson, K.Y., Hughes, D.J., Thurston, P.C., Hall, R.P., 1999. Plume magmatism and crustal growth at 2.9 to 3.0 Ga in the Steep Rock and Lumby Lake area, Western Superior Province. Lithos 46, 103–136.

Tomlinson, K.Y., Condie, K.C., 2001. Archean mantle plumes: evidence from greenstone belt geochemistry. In: Ernst, R.E., Buchan, K.L. (Eds.), Mantle Plumes: Their Identification through Time. Geol. Soc. Am. Spec. Pap. 352, 341–357.

Tomlinson, K.Y., Davis, D.W., Percival, J.A., Hughes, D.J., Thurston, P.C., 2002. Mafic to felsic magmatism and crustal recycling in the Obonga Lake greenstone belt, western Superior Province: evidence from geochemistry, Nd isotopes and U-Pb geochronology. Precambrian Res. 114, 295–325.

Volpe, A.M., Macdougall, J.D., Hawkins, J.W., 1987. Mariana Trough basalt (MTB): trace element and Sr-Nd isotopic evidence for mixing between MORB-like and arc-like melts. Earth Planet. Sci. Lett. 82, 241–254.

Volpe, A.M., Macdougall, J.D., Hawkins, J.W., 1988. Lau basin basalt (LBB): trace element and Sr-Nd isotopic evidence for heterogeneity in backarc basin mantle. Earth Planet. Sci. Lett. 90, 174–186.

Wang, Z., Wilde, S.A., Wang, K., Yu, L., 2004. A MORB-arc basalt-adakite association in the 2.5 Ga Wutai greenstone belt: late Archean magmatism and crustal growth in the North China craton. Precambrian Res. 131, 323–343.

Winchester, J.A., Floyd, P.A., 1977. Geochemical discrimination of different magma series and their differentiation products using immobile elements. Chem. Geol. 20, 325–343.

White, R.V., Tarney, J., Kerr, A.C., Saunders, A.D., Kempton, P.D., Pringle, M.S., Klaver, G.T., 1999. Modification of an oceanic plateau, Aruba, Dutch Caribbean: implications for the generation of continental crust. Lithos 46, 43–68.

de Wit, M.J., 1998. On Archean granite, greenstones, cratons and tectonics: does the evidence demant a verdict. Precambrian Res. 91, 181–226.

Wood, D.A., Joron, J.L., Treuil, M., 1979. A re-appraisal of the use of trace elements to classify and discriminate between magma series erupted in different tectonic settings. Earth Planet. Sci. Lett. 50, 326–336.

Wood, D.A., Marsh, N.G., Tarney, J., Joron, J.L., Fryer, P., Treuil, M., 1981. Geochemistry of igneous rocks recovered from a transect across the Mariana Trough, Arc, Fore-arc, and Trench, sites 453 through 461, Deep Sea Drilling Project Leg 60. In: Hussong, D.M., Uyeda, S., et al. (Eds.), Init. Rep. Deep Sea Drill. Proj. 60, 611–645.

Wyman, D.A., 1999. A 2.7 Ga depleted tholeiite suite: evidence of plume-arc interaction in the Abitibi greenstone belt, Canada. Precambrian Res. 97, 27–42.

Wyman, D., Hollings, P., 1998. Long-lived mantle-plume influence on an Archean protocontinent: geochemical evidence from the 3 Ga Lumby Lake greenstone belt, Ontario, Canada. Geology 26, 719–722.

Wyman, D.A., Bleeker, W., Kerrich, R., 1999. A 2.7 Ga komatiite, low Ti tholeiite, arc tholeiite transition, and inferred proto-arc geodynamic setting of the Kidd Creek deposit: evidence from precise trace element data. Econ. Geol. Monogr. 10, 511–528.

Wyman, D.A., Kerrich, R., Polat, A., 2002. Assembly of Archean cratonic mantle lithosphere and crust: plume-arc interaction in the Abitibi-Wawa subduction-accretion complex. Precambrian Res. 115, 37–62.